UNIVERSITY OF LEEDS

This is a repository copy of *Sky islands as foci for divergence of fig trees and their pollinators in southwest China*.

White Rose Research Online URL for this paper:
http://eprints.whiterose.ac.uk/156139/

Version: Accepted Version

Article:

Deng, J, Fu, R, Compton, SG orcid.org/0000-0002-1247-8058 et al. (5 more authors) (2020) Sky islands as foci for divergence of fig trees and their pollinators in southwest China. Molecular Ecology, 29 (4). pp. 762-782. ISSN 0962-1083

https://doi.org/10.1111/mec.15353

© 2020 John Wiley & Sons Ltd. This is the post-peer reviewed version of the following article: Deng, J-Y, Fu, R-H, Compton, SG, et al. Sky islands as foci for divergence of fig trees and their pollinators in southwest China. Mol Ecol. 2020; 29: 762– 782. which has been published in final form at https://doi.org/10.1111/mec.15353. This article may be used for non-commercial purposes in accordance with Wiley Terms and Conditions for Use of Self-Archived Versions.

Reuse
Items deposited in White Rose Research Online are protected by copyright, with all rights reserved unless indicated otherwise. They may be downloaded and/or printed for private study, or other acts as permitted by national copyright laws. The publisher or other rights holders may allow further reproduction and re-use of the full text version. This is indicated by the licence information on the White Rose Research Online record for the item.

Takedown
If you consider content in White Rose Research Online to be in breach of UK law, please notify us by emailing eprints@whiterose.ac.uk including the URL of the record and the reason for the withdrawal request.

White Rose
university consortium
Universities of Leeds, Sheffield & York

eprints@whiterose.ac.uk
https://eprints.whiterose.ac.uk/

Sky islands as foci for divergence of fig trees and their pollinators in South-West China

Jun-Yin Deng [1, 3 #], Rong-Hua Fu[1#], Stephen G. Compton[2], Mei Liu[1], Qin Wang[1], Chuan Yuan[1], Lu-Shui Zhang[1], Yan Chen[1]*

1 Ecological Security and Protection Key laboratory of Sichuan Province, Mianyang Normal University, Mianyang, Sichuan 621000, China

2 School of Biology, University of Leeds, Leeds LS2 9JT, United Kingdom

3 Department of Genetics, University of Pretoria, Pretoria 0002, South Africa

Co-first author

*Author for correspondence:

Yan Chen

Ecological Security and Protection Key Laboratory of Sichuan Province,

Mianyang Normal University

Mianyang, Sichuan 621000

China

Email: goose_01@163.com

Abstract

The dynamics of populations and their divergence over time have shaped current levels of biodiversity and in the case of the 'sky islands' of mountainous SW China have resulted in an area of exceptional botanical diversity. *Ficus tikoua* is a prostrate fig tree sub-endemic to the area that displays unique intraspecific diversity, producing figs typical of different pollination modes in different parts of its range. By combining climate models, genetic variation in populations of the tree's obligate fig wasp pollinators and distributions of the different plant phenotypes, we examined how this unusual situation may have developed. We identified three genetically distinct groups of a single *Ceratosolen* pollinator species that have largely parapatric distributions. The complex topography of the region contributed to genetic divergence among the pollinators by facilitating geographic isolation and providing refugia. Migration along elevations in response to climate oscillations further enhanced genetic differentiation of the three pollinator groups. Their distributions loosely correspond to the distributions of the functionally significant morphological differences in the male figs of their host plants, but postglacial expansion of one group has not been matched by spread of its associated plant phenotype, possibly due to a major river barrier. The results highlight how interplay between the complex topography of the 'sky-island' complex and climate change has shaped intra-species differentiation and relationship between the plant and its pollinator. Similar processes may explain the exceptional botanical diversity of SW China.

Key words: Agaonidae, *Ficus*, fig wasp, glacial refugia, pollination

Introduction

Factors that shape the dynamics of populations and their divergence over time have combined to determine current levels of biodiversity (Avise, 2000). Among those factors, tectonic activities have played an important role in the genesis of biodiversity because they can create geographic dispersal barriers such as mountain ranges or major river systems that isolate populations and lead to species diversification (Zhang et al., 2007; Cheng et al., 2016; Achimon et al., 2018; Yu et al., 2019a). Climate oscillations, especially the Quaternary glacial-interglacial cycles, are also seen as drivers of population divergence (Ibrahim et al., 1996) when retreat to glacial refugia generates fragmentation and isolation facilitates divergence and speciation (Hewitt, 2000; 2004). In the northern hemisphere, species typically retreat towards southern refugia during glacial periods and expand northwards in response to the warmer conditions of inter-glacials. Genetic divergence among populations centered on different refugia has been described frequently, but phenotypic variation and its associated selection pressures are less well documented (Margraf et al., 2007; McCormack & Smith, 2008; Mayol et al., 2015; Polfus et al., 2017).

Terrestrial biodiversity varies with elevation as well as latitude (Lomolino, 2001; Willig et al., 2003; Grytnes & Mccain, 2007). Together with latitudinal shifts in distribution, climate change also modifies the altitudinal ranges that species occupy, with cold-adapted montane species expanding their ranges to lower elevations during glacial periods and retreating higher during inter-glacials. Consequently, species currently distributed across high elevation habitats are likely to have exhibited more extensive gene flow between populations at colder times in the past. Such cycles of expansion and retreat have shaped genetic divergence between populations of montane species as well as influencing their distribution patterns. Higher elevation regions of major mountain ranges have been termed as 'sky islands' to reflect this (Heald, 1951; McLaughlin, 1994; He & Jiang, 2014). Within the broad pattern of montane species expanding their ranges to lower elevations during glacial periods, cyclic changes in distribution are not necessarily simple, and the complex topography and microclimates of large mountain ranges can provide refugia for different species in different places (Davis & Shaw, 2001; Haubrich & Schmitt, 2007; Chen et al., 2012; Qiu et al., 2011; Sharma et al., 2014). Mountains are therefore often centers of endemism and species diversity hotpots (Rafiqpoor et al., 2005; Noroozi et al., 2018; Zhou et al., 2018), as well as foci for divergence between populations of the same species that have become isolated on different mountains (Myers et al., 2000; Barthlott et al., 2005; Popp et al., 2008; Xu et al., 2016).

The uplift of the Qinghai–Tibet Plateau (QTP) in East Asia created major mountain ranges across adjacent southwestern China (Favre et al., 2015). This complex of sky islands has been recognized recently as a major contributor to the extremely high biodiversity of this area, but the interplay between the mountains, climate changes and the species-specific responses they have generated is largely unknown (He & Jiang, 2014). He & Jiang (2014) defined the Southwest China sky-island complex as comprising the Hengduan Mountains, the Yun-Gui Plateau and the mountains surrounding the Sichuan Basin. They form part of the Sino-Himalayan Forest subkingdom, which harbors a famously diverse temperate flora (Qiu et al., 2011). The uplift of the QTP will have generated both mountain ranges and new river systems that can have acted as barriers to dispersal and the isolation of populations of species inhabiting the area. These, together with climate cycles and the varying elevations of the mountains are likely to have combined to facilitate divergence among populations of many of these species (Hewitt, 2004), though their individual responses will have varied depending on their autecology. Reflecting this, for different species, the sky islands and their associated river systems will have acted to varying extents as barriers to gene flow that facilitated population divergence (Fan et al., 2012; Liu et al., 2012), while also providing dispersal corridors for other species (Zhang et al., 2010; Qu et al., 2011).

Most biological studies in this region have focused on temperate or alpine species, with little attention paid to subtropical species at their northern boundaries, but mountain ranges are known to have driven divergence among both tropical and temperate species (Hewitt, 2004). Fig trees (*Ficus* species, Moraceae) are distributed mostly in tropical and subtropical regions, but a few species extend naturally into temperate areas of China, where their distributions have been shown to have ebbed and flowed in response to glacial cycles (Chen et al., 2012). Factors determining the northern and altitudinal range boundaries of fig trees are poorly understood. More seasonal and cold conditions are not necessarily the factors that directly limit their distributions, because several widely-planted species grow successfully much further north than their natural ranges (Wang et al., 2015a). Limitations to the plants' ability to reproduce in highly seasonal climates are a likely contributor, because reproduction depends on the behavior and survival of their fig wasp pollinators (Hymenoptera, Agaonidae). This has required most extra-tropical fig tree species in China and Europe to modify their life cycles to allow pollinator larvae to survive the winter months inside their figs (Valdeyron & Lloyd, 1979; Zhang et al., 2014; Zhao et al., 2014).

Fig trees are pollinated exclusively by host-tree-specific fig wasps and consequently the distributions of the plants and insects are intimately linked (Herre et al., 2008; Liu et al., 2014). Figs are the highly specialized enclosed inflorescences of *Ficus* species. Adult female fig wasps transfer pollen after they enter each fig via a narrow entrance hole (the ostiole). The female fig wasps enter the figs to lay their eggs inside the ovules that line their inner surface. They also gall these ovules. Fig wasps are small (less than three mm) and live as adults for only one to two days after emerging from their natal figs (Ware & Compton, 1994), during which time they are highly vulnerable to abiotic stresses (Jevanandam et al., 2013). Despite these constraints, some fig wasps disperse considerable distances between host trees, using the wind to carry them (Compton et al. 2000; Ahmed et al., 2009; Nazareno et al., 2013).

Ficus tikoua Bur. is a small species of dioecious fig tree with a limited range centered on warm-temperate Southwest China. It has a largely montane distribution that is closely associated with the region’s sky island centres of botanical diversity (Fig. 1). Within its large genus, *F. tikoua* is exceptional in terms of the variation it exhibits in inflorescence composition. Deng et al. (2016) identified three types of male flower distributions inside its male figs. They contain either small numbers of male flowers concentrated around the ostioles (ostiolar type) or larger numbers of flowers scattered throughout the figs (scattered type). A few individuals have an intermediate condition, with small numbers of scattered male flowers (intermediate type) (Deng et al., 2016). The presence of small numbers of male flowers in figs is associated with active pollination behavior where pollinator females collect pollen from their natal figs into thoracic pockets and then unload the pollen in the figs where they lay their eggs. This is more efficient than the passive transfer of pollen and actively-pollinated *Ficus* species benefit by being able to greatly reduce the number of male flowers present in their figs, in comparison with species with pollinators that pollinate passively (Kjellberg et al., 2001). Active pollination behavior favours pollinator larval development because it helps ensure that the flowers where larval develop have been both pollinated and galled. The flowers in female figs have more exposed stigmas than those in male figs. This means that they can come into contact more effectively with pollen located on the bodies of fig wasps, but fig wasps that disperse pollen passively lack control over which flowers are pollinated.

The variation in male flower numbers in figs of *F. tikoua* suggests that in some areas the plant is actively-pollinated, and that pollination in other areas might be passive. Active pollination might be supplemented by passive pollination in the areas where many male flowers are present in the figs, depending on the behaviour of the pollinators. The known pollinator of *F. tikoua* is an undescribed species of *Ceratosolen* (Cruaud et al., 2012; Deng et al., 2016). Almost all *Ceratosolen* species are believed to be active pollinators, because they possess the coxal combs and pollen pockets that are used to manipulate and store pollen (Kjellberg et al., 2001; Deng et al., 2016). One

African *Ceratosolen* species has reduced pollen pockets and no longer pollinates its hosts (Compton et al., 1991), but the species associated with *F. tikoua* consistently has functional pollen pockets that contain pollen, suggesting it is an active pollinator, despite the observed variation in its host figs (Deng et al., 2016).

Here, we use the population genetic structure of the *Ceratosolen* pollinator of *F. tikoua* in combination with the distribution of differing inflorescence phenotypes of the plant to examine the phylogeography of their association and its relationship with changes in distribution resulting from Pleistocene climate change (Fig. 2). Specifically, we ask (1) What is the extent of genetic divergence among populations of the fig wasp and does it indicate that more than one species is present? (2) What are the current distributions of pollinator genetic groups and can their divergence be related to geographic isolation caused by QTP uplift and the changes in climate that have resulted in the distribution of their largely montane host plant expanding and contracting over time? (3) Does geographical variation in male flower numbers inside the figs of *F. tikoua* correspond to the distributions of genetically distinct populations of the pollinator?

Materials and Methods

Natural History

Ficus tikoua is a dioecious fig tree placed in subgenus *Sycomorus* (Cruaud et al., 2012). Its distribution extends across Southwest China and montane areas of Laos, North India and North Vietnam (Zheng et al., 1978). According to the Chinese Virtual Herbarium (http://www.cvh.ac.cn/) and Global Biodiversity Information Facility (https://www.gbif.org/) the distribution of the plant in China extends across and around the Sichuan Basin, the Hengduan Mountains and the Yungui Plateau (the area of Southwest China referred to as the sky-island complex, Fig. 1). *F. tikoua* is a species of open habitats including disturbed land, rocky areas and open woodland and occurs at a range of elevations from 200-2600 m. It is a prostrate creeping shrub that rarely exceeds 30 cm in height. The figs are located close to or partially buried in the soil. The mature female figs are aromatic, light brown and reach about 2 cm in diameter. The animals that disperse the seeds are unknown, but the position, appearance and fragrance of the figs suggest they are likely to attract terrestrial mammals, rather than fruit-eating birds or bats. The distance its seeds are dispersed may therefore be limited. The known pollinator of *F. tikoua* belongs to the genus *Ceratosolen* (Cruaud et al., 2012, Deng et al., 2016). Some *Ceratosolen* species routinely disperse pollen over large distances and consequently have host populations that display limited genetic structuring (Ahmed et al., 2009, Kobmoo et al., 2010, Bain et al., 2016). The dispersal distances of the *Ceratosolen* pollinator of *F. tikoua* appears to be more limited because the population genetic structure of the plant suggests highly restricted gene flow, with significant differentiation between populations separated by as little as 31 km (Chen et al., 2011).

Sampling

Insects from different sample sites were regarded as representing different populations. A total of 48 natural populations of the pollinating fig wasp of *F. tikoua* were sampled between May 2013 and May 2015 across Southwest China (Fig. 1, Table 1). Because of the creeping, prostrate habit of the plant, it is often difficult to distinguish individual plants. Figs ascribed to a single male host plant were therefore collected within defined areas of 1m^2. The samples were separated by at least 30 m to prevent repeat sampling of the same individuals. Mature figs containing fig wasp adult offspring were removed and placed separately in fine-mesh bags to let wasps emerge naturally. The figs were then cut in half and the distribution patterns of their male flowers were recorded as either ostiolar, scattered or intermediate (Deng et al., 2016). The fig wasps that emerged from the figs were stored in ethanol at 4° C. Distribution records from Deng et al. (2016) were combined with results from these surveys to map the distribution of plants with different male flower patterns.

DNA extraction, sequencing and genotyping

Females were chosen at random from those that emerged from each fig. We used about 10 fig wasps for sequencing COI and ITS2 and 20 for SSR genotyping in each population. Mostly, one female fig wasp was used per fig in every population, but two to three individuals from a single fig were used when insufficient source figs were available (Table 1). More than one foundress may produce offspring within shared figs of *F. tikoua*. We compared the relatedness of fig wasps from the same fig and different figs based on their microsatellite genotypes. No significant differences were detected between the two groups (Fig. S1).

The genomic DNA of the fig wasps was extracted from individual females using the method of Sambrook et al. (1989), which digests the protein with proteinase K, lyses the cells with Sodium dodecyl sulfate (SDS), then extracts, precipitates and purifies the DNA with Chloroform-isoamyl alcohol, isopropanol and alcohol. The mitochondrial COI and nuclear ITS2 genes were sequenced using the primers LCO1490/HCO2198 (Folmer et al., 1994) and ITSF/ITSR (Lopez-Vaamonde et al., 2001) respectively, following the procedures in Chen et al. (2012). Six to ten individuals were sequenced from two directions for both genes in each population (Table 1). The reliability of all the COI and ITS2 sequences was checked and only the sequences with unambiguous chromatograms in both directions were used. The COI genes were translated into protein sequences to check for stop codons and frame-shifting mutations with MEGA 5 (Tamura et al., 2011), using the invertebrate mitochondrial genetic code.

The nuclear microsatellite genotypes were scored using specific microsatellite primers developed for the *Ceratosolen* sp. associated with *F. tikoua* (C35, C54, C101, C113, C114, C149, C160, C175, C202, C234), following the methods of Tan et al. (2016). Seven to 31 wasps were used for each population. The linkage disequilibrium (LD) between each pair of loci was tested with FSTAT 2.9.3 (Goudet, 2001), and selection on each locus was tested with a stepwise mutation model (SMM) using LOSITAN (http://popgen.net/soft/lositan/). Only independent loci that had undergone no positive selection were used in the subsequent analyses.

Genetic divergences and geographic distributions

Networks were constructed using COI and ITS2 sequences of all sampled individuals with TCS 1.21 and a 95% connection limit statistical criterion (Clement et al., 2000). The GenBank sequence of the *F. tikoua* pollinator (JN103257, which was collected in Wuding County, close to the location of our YWD population, J-Y. Rasplus personal comm.) was also included when the COI network was assembled.

The phylogenetic relationships and divergence time of the *Ceratosolen* sp. were reconstructed based on COI sequences, using BEAST 2.4.3 (Bouckaert et al., 2014) with best substitution models, using Bayesian Markov chain Monte Carlo (MCMC) analysis. We included nine species from the genera *Ceratosolen* (6) and *Kradibia* (3) as outgroups in the phylogenetic analysis. The substitution model was tested with JMODELTEST, and GTR+I+G was chosen based on the AIC criterion. Strict clock, uncorrelated exponential relaxed clock and uncorrelated lognormal relaxed clocks were tried with a birth-death population growth model. We used the published 59.7 (75.4-43.3) Ma age for the crown group of the genus *Ceratosolen* for divergence time estimation under a uniform distribution (Cruaud et al., 2012). We specified all *Ceratosolen* as a monophyletic ingroup with the root between *Ceratosolen* and *Kradibia* and ran 10 million MCMC and sampled every 10 000 generations to estimate posterior distributions of parameters. TRACER 1.5 (Rambaut & Drummond, 2009) was performed to check the convergence of the parameters sampled, which was based on effective sample sizes (ESSs). All ESSs for every parameter had to be larger than 200. Bayes factors were calculated in TRACER to tell the best clock model. A strict clock was selected based on Bayes factors ($\ln BF = 28.452 \pm 0.035$). Then two independent runs were performed with the parameters kept the same as before. The results of the two runs were combined by LOGCOMBINER (Bouckaert et al., 2014). TREEANNOTATOR was used to search the maximum clade credibility tree with 10%

"burn-in". The final tree was visualized in FIGTREE 1.4.2 (http://tree.bio.ed.ac.uk/software/figtree/), with the genetic clades then identified based on the phylogenetic trees.

We only performed basic analysis on ITS due to its slow rate of divergence. The phylogenetic relationships of ITS2 genes were built by two methods. The Bayesian tree was constructed in MRBAYES 3.2.4 (Ronquist et al., 2012) under a F81 model, which was selected based on AIC criteria using JMODELTEST 2.1.7 (Darriba et al., 2012). The Maximum Parsimony tree was built using PAUP 4.0 (Swofford, 2002). We failed to obtain any outgroups for our ITS2 data sets, so we did all the phylogenetic trees without outgroups.

Genetic differentiation of SSR genotypes was assessed using a Bayesian approach implemented in STRUCTURE 2.3.4 (Pritchard et al., 2000). Twenty runs were performed for each K from K = 1 to K = 10, with 10 000 burn-ins and 100 000 MCMC repetitions for each run. ΔK values was assessed on the website of STRUCTURE HARVESTER (Earl & vonHoldt, 2012), and were used to detect the optimal K number (Evanno et al., 2005). The sampled individuals were then assigned to each group, ignoring their geographic coordinates. Two independent runs were performed with 30 000 burn-ins and 1 000 000 MCMC repetitions.

Genetic discontinuities between population pairs were explored using BARRIER 2.2 (Manni et al., 2004) with Monmonier's maximum-difference algorithm based on the SSR components of each population. One thousand Nei's genetic distance matrices were used to estimate the robustness of gene flow barriers. Nei's genetic distance matrices were produced by bootstrapping loci with MICROSATELLITE ANALYSER 4.05 (MSA; Dieringer & Schlötterer, 2003). The genetic groups were distinguished based on genetic discontinuities, and were then compared with genetic clades identified by the COI tree.

Differentiation within and among defined groups was tested by an analysis of molecular variance (AMOVA) using ARLEQUIN 3.5 (Excoffier & Lischer, 2010) with 1 000 permutations, based on both COI and SSR data. Pairwise genetic differentiation between populations were assessed based on SSR data using FSTAT (Goudet, 2001) with 1 000 permutations, applying sequential Bonferroni corrections.

To identify the role of geographic distance in genetic differentiation, the isolation by distance (IBD) pattern was assessed by Mantel tests using SSR data. The regression of pairwise estimates of genetic distances F_{ST} / (1- F_{ST}) against the corresponding geographic distance was conducted using the R 3.3 package 'Vegan' (http://www.r-project.org/). One thousand permutations were used to determine statistical significance. The tests were performed on all sampling regions and the separate geographic regions of each genetic group.

Genetic diversities of each population and genetic group

For COI and ITS2 data, the genetic diversities of each group and population were assessed using the number of haplotypes (h), average numbers of nucleotide diversity (k), haplotype diversity (Hd) and nucleotide diversity (π), using DNASP 5.10 (Librado & Rozas, 2009). The genetic distances within and between genetic clades were calculated by MEGA.

For SSR data, the deviations from Hardy-Weinberg equilibrium (*HWE*) in each population were examined by the multi-loci exact test in GENEPOP 4.0 (Rousset, 2008). A Markov chain method was used to estimate the *P* value of the test. The number of alleles (*Na*), observed (H_O) and unbiased expected heterozygosity (H_E) were calculated using FSTAT. The allelic richness (A_R) after rarefaction due to different sample sizes between populations, and average number of private alleles per locus were calculated using HP-RARE (Kalinowski, 2005). Inbreeding coefficients (F_{IS}) for each population and global genetic differentiation were estimated with 1 000 permutations in FSTAT.

Demographic history of each genetic group

The genetic clades were defined with a COI phylogenetic tree. The demographic dynamics of genetic clades recognized by earlier analyses were examined based on COI sequences of all sampled individuals. The mismatch distributions under both the sudden expansion and spatial expansion models for each clade were analyzed using ARLEQUIN. *Tajima's D* and *Fu's Fs* were tested to further infer their population history, again using ARLEQUIN. The demographic dynamics at different times were explored by Bayesian Skyline Plot analysis (BSP) performed in BEAST. The best substitution model was calculated using JMODELTEST. We tried both an uncorrelated exponential relaxed clock and an uncorrelated lognormal relaxed clock. A uniform distribution of substitutions over time was assumed for estimating expansion times with a lower substitution rate of 1.2% per Ma and an upper substitution rate of 2.8% per Ma (based on typical substitution rates of COI genes for insects, Molbo et al., 2003). Bayes factors were calculated to select the most suitable molecular clock under the most likely substitution model. We ran MCMC with 20 000 000 steps and sampled every 2 000 steps. Convergence in each run was checked using TRACER. The run length was increased until the ESSs of all parameters were above 200. Then Bayesian skyline plots were generated with a 10% burn-in by TRACER.

The genetic groups were defined by genetic discontinuities as well as the STRUCTURE assignment based on the SSR data set. The demographic histories of genetic groups were also inferred through a two-step ABC (approximate Bayesian computation) approach, which was performed with DIYABC (Cornuet et al., 2014) using SSR data. The three groups were regarded as different populations, as required by DIYABC. First, we tested each of five demographic scenarios to find out the most likely option. Then we re-ran DIYABC considering different ancestral groups based on the best scenario identified by the first run. The specific scenario settings for the first and second runs are shown in Fig. S2 and Fig. S3. Generalized stepwise mutation models (SMM) for SSRs with the higher and lower mutation rates were explored. All parameters were set by default prior values, with 100 000 simulations performed for each scenario. The goodness of fit of each scenario was assessed by the principal component analysis (PCA) option "model checking" in DIYABC, which measures how close the simulated datasets are to the real datasets. Posterior probabilities were evaluated using both direct and logistic approach in order to select the most likely scenario.

The historical distribution of the host plant

Species Distribution Models (SDM) were used to simulate the most probable distributions of *F. tikoua* populations at the end of the last interglacial period (LIG, *c*. 120 ka BP) and the last glacial maximum (LGM, *c*. 20 ka BP). The current distributions of *F. tikoua* in China were obtained from records in the Chinese Virtual Herbarium (CVH, http://www.cvh.ac.cn/), Global Biodiversity Information Facility (GBIF, https://www.gbif.org/) and from our field collections. These provided a total of 535 confirmed locations of the plant (after excluding some wrongly identified specimens). Current, LIG and LGM climatic variables were downloaded from WorldClim at 2.5 arc-min, 30 arc-seconds and 2.5 arc-min resolutions, respectively (http://www.worldclim.org/). Paleoclimatic data at LGM were simulated by the community climate system model (CCSM) (Collins et al., 2006). Current and historical SDMs were performed using maximum entropy algorithms in MAXENT 3.4.1 (Phillips & Dudík, 2008) by combining current distribution records with current and historical climatic estimates. We constructed the final models with ten cross-validation replicates. The consistency of model predictions of species distributions during different periods were measured based on AUC (Areas Under Curves, a good indicator for model performance, with values > 0.9 indicating high-accuracy models). A summary figure of the simulated results was then generated in ARCGIS 10.2 (http://www.esri.com/). The characteristics (latitude, longitude and elevation) of the most suitable areas (with SDM values of predicted probability greater than 0.8) during the three periods were extracted using ARCGIS 10.2. Boxplot figures of each parameter during each period were drawn in R. Differences in distributions were compared using Tukeys HSD multiple comparison tests in R.

Climate data analysis

We obtained 19 climate variables covering the LIG, LGM, and current periods from WorldClim (http://www.worldclim.org/) (Table S1) and extracted them based on our sample sites using ARCGIS (http://www.esri.com/) (Table 1). The means and standard errors of these climate variables during different time periods were calculated for groups of populations assigned to particular genetic groups using Microsoft Excel. Tukeys HSD multiple comparison tests, conducted in R, were used to compare climate variables at different times within each region.

The relationship between male flower distribution in plant hosts and the genetic structure of their pollinators

We used chi-square tests to examine the relationship between different host male flower distribution phenotypes and the genetic structure of pollinators using Monte Carlo tests with 2000 replicates to obtain probabilities. The 3x4 contingency tables had columns representing populations displaying either ostiolar only, scattered only or mixed floral phenotypes, and rows numbering populations with only a single genetic group or a mixed genetic signal (based on the nSSR clusters and the COI phylogeny tree).

Results

The sequenced COI gene from *Ceratosolen* sp. was 666 bp long. Four hundred and sixty-seven unambiguous sequences were obtained from the 48 populations of the insect (Fig. 1, Table 1) from which 69 haplotypes were distinguished. No signs of mitochondrial pseudogenes were detected in any of the 69 COI haplotypes (GenBank Accession Number: MK241697-241765). They displayed no frame shifts and stop codons when translated into protein chains using the invertebrate mitochondrial genetic code. Most substitutions were in the third codon position (97%), and most were synonymous mutations (97%).

The fragments of ITS2 were 677 bp long, from which 448 sequences and 18 haplotypes were obtained (GenBank Accession Number: MK241766-241783), with 9 insertions or deletions present (Table 1).

Multiple loci SSR genotypes of 1104 wasps were scanned (Table 1). No linkage disequilibria were detected between pairs of SSR loci, but one locus (C149) was under positive selection and not included in subsequent analyses. Any populations with less than ten individuals were also excluded. This left 1082 individuals from 45 populations (Table 1).

Divergence between populations

Both COI and ITS2 divided *Ceratosolen* sp. into three monophyletic clades (Fig. 3 and Fig. S4). The Bayesian tree and network of the COI sequences divided the pollinating fig wasps from *F. tikoua* into three monophyletic clades (the red, yellow and blue clades in subsequent figures), with the three genetic clades linked together in the network based on the 95% statistical criterion (Fig. 3). The COI sequence of the *Ceratosolen* sp. from *F. tikoua* in GenBank (JN103257) is the most common haplotype of the yellow clade (C13). Three monophyletic clades were also supported by the phylogenetic tree of ITS2 sequences (Fig. S4). The Blue clade could not be connected to the other clades under the 95% statistical criterion in the ITS2 network, whereas all three clades were linked together in the COI network (Fig. S4). The average K_2P distances of COI sequences within and between the three clades were 0.66% (0.47-0.88%) and 2.24% (1.72-2.84) respectively.

Pliocene divergence times were indicated by the COI Bayesian tree, with the blue clade splitting from the other two clades first, about 5.01 Ma (95% HPD: 2.89-7.43 Ma), and the red and yellow clades diverging from each other about 3.53 Ma (95% HPD: 1.89-5.35 Ma) (Fig. 3). The phylogenetic placements based on the COI and ITS2 genes were usually consistent, but two common ITS2 haplotypes included fig wasps from different COI clades (I08, including the blue and yellow COI clades; I10, including the red and yellow COI clades) (Fig. S4).

When genetic groups based on microsatellite data were assessed, ΔK values supported the presence of two groups (Fig. S5). To compare the individuals belonging to SSR groups with those of COI and ITS2 clades, K was set to both 2 and 3 when the SSR memberships was assigned by STRUCTURE. Most individuals were assigned to just one group, however some individuals displayed multiple-group placements (Fig. 4). When K was set to 2, the individual components of the two SSR groups were generally equivalent to the constituents of the blue and the red plus yellow COI clades (Fig. S6).

When three groups were set (K = 3), the genetic components of most individuals were again in agreement with the three COI clades (Fig. 5). The genetic assignments of each individual were also provided in Fig. S7, with k being set from four to ten.

Geographic distributions of pollinator genetic clades

The three clades defined by the COI genes had largely allopatric distributions, with the blue clade in the south and south east, concentrated on the Yungui Plateau (YGP), the yellow clade located to the west in the Hengduan Mountains (HDM) and the red clade to the north in and around the Sichuan Basin (SCB). The geographic distributions of the COI clades were generally concordant with the regional distribution of SSR groups. When two SSR groups were set, one genetic group covered SCB and HDM, while another group was distributed mostly on YGP (Fig. S6). When three groups were set, the three groups were again each concentrated in the SCB, HDM and YGP areas. However, a few populations, mostly located in the contact zones between genetic groups, had individuals with multiple SSR component groups (82 individuals out of 1104). In order to assign those populations to one of the genetic groups, barriers to gene flow were assessed based on SSR data. Strong genetic discontinuities were identified, and they again defined three geographic regions, which matched well with the geographic distribution of both the COI clades and SSR groups (Fig. 5). Consequently, the genetic groups of pollinating fig wasp of *F. tikoua* based on SSR were defined by genetic discontinuities into three (YGP-, HDM- and SCB- located) genetic groups. Each of these groups containing mainly individuals from one genetic clade, but with a small number of individuals from other genetic groups (Figs. 4 & 5). AMOVA detected significant differentiation among the three COI clades and among the SSR groups (ϕ_{SC} = 0.425, $p < 0.001$ for COI; $F_{SC} = 0.232$, $p < 0.001$ for SSR). The COI haplotypes had different frequencies in the three regions. SCB and HDM each had just one common haplotype (C03 in SCB, C13 in HDM), whereas YGP had three common haplotypes (C10, C46, C50) (Table 1, the network in Fig. S4).

Isolation by distance (IBD) patterns showed that geographic distance played a considerable role in the differentiation of populations. Significant relationships between genetic distances (F_{ST} / (1- F_{ST})) and geographic distances were detected when all populations were pooled together (r = 0.411, $p < 0.001$, Fig. S8), or when the HDM (r = 0.273, $p = 0.046$) and YGP populations (r = 0.508, $p < 0.001$) were considered separately (Fig. S9). However, no significant IBD pattern was detected in the SCB populations (r = 0.174, $p = 0.083$, Fig. S9). The global F_{ST} based on SSR data was 0.317 ($p < 0.05$), and the YGP, HDM and SCB F_{ST} were 0.188 ($p < 0.05$), 0.260 ($p < 0.05$), 0.241 ($p < 0.05$), respectively. Significant differences between almost all pairs of populations were shown by pair-wise F_{ST} values based on SSR data (981 out of 990 population pairs, Table S2).

Demographic histories of the three Ceratosolen *sp. clades*

Different demographic historical dynamics were detected among the three *Ceratosolen* sp. clades. The COI network of the red clade showed a star-like topology with all the haplotypes connecting to the most common haplotype (C03) by no more than five mutations. Such a star-like network often indicates recent population expansion (Mirol et al., 2008). More complicated topologies were revealed in the yellow and blue clades. The most common haplotype of the yellow clade (C13) did not form the core of its network and the three common haplotypes in the blue clade (C10, C46, C50), formed three individual star-like networks connected to each other.

Differences in expansion patterns in the three pollinator clades were further suggested by mismatch and neutrality tests. Significant expansion in the red clade was supported (*Fu's Fs* = -7.099, $p = 0.011$; p (SSD) > 0.05 for simulations under both sudden and spatial expansion models). Although mismatch distribution analysis suggested recent spatial expansion in all three clades, expansion in the yellow clade was rejected by *Fu's Fs* ($p = 0.133$). This was confirmed by the mismatch distribution under a sudden expansion model (p (SSD) < 0.001). For the blue clade, recent expansion was indicated by *Fu's Fs* ($p = 0.023$), but rejected by the simulation under a sudden expansion model (p (SSD) = 0.011) (Table 2).

Tajima's D did not vary significantly from zero in all three clades, suggesting there have been no recent bottlenecks (Tajima, 1989). Bayesian Skyline Plot analysis showed a demographic expansion in the blue clade about 15 ka BP, but effective population sizes were found to have remained stable in the red and yellow clades (Fig. 6).

The historical divergence dynamics of the three groups defined by genetic discontinuities were concordant with the topology of the COI phylogenetic trees. When divergence history was tested by DIYABC, based on the SSR data, the best supported scenario revealed that genetic group HDM has retained ancestral genetic components, with YGP diverging first, then SCB (posterior probabilities were 0.929 and 0.878 for the first and second DIYABC runs respectively) (Fig. S3, Fig. S4).

Simulated historical distribution patterns of Ficus tikoua

The SDM model provided a good fit to the contemporary geographic distribution of *F. tikoua* and generated realistic simulations of its historical distributions. The AUC values for the replicate runs were 0.907 ± 0.005, 0.905 ± 0.005, 0.913 ± 0.005 for the modern day, last interglacial period and last glacial maximum respectively. The models suggest that *F. tikoua* has remained in southwest China throughout the last 120 ka BP, but within this area has had different distribution patterns at different times. During the last interglacial, three well-supported areas of distribution (with a predicted probability of occurrence above 0.8) were identified in the three mountain areas that are also most suitable for the plant today. This distribution pattern is consistent with the barriers to gene flow of its pollinators based on SSR (Fig. 7). An area with suitable climate acted as a bridge between the Hengduan Mountains and Sichuan Basin, but the Yungui Plateau area of distribution was more isolated (Fig. 7a, Fig. 8). At the last glacial maximum the area suitable for the distribution of *F. tikoua* moved in a Northeastern direction to lower-elevation regions (Fig. 7b, Fig. 8). Most of the area in the SW of the plant's current distribution, the area currently occupied mainly by the yellow pollinator clade, became unsuitable at that time. In contrast, the area of suitable habitat further north, where the red clade is concentrated today, increased. The area to the SE currently occupied mainly by the blue clade moved northwards at LGM, and declined in extent. After the glacial period, areas in the SW became more suitable again.

The modeled movement of *F. tikoua* to lower elevations between the LIG and LGM and its subsequent return to higher elevations as seen in the present day are reflected in changes in the estimated mean elevations of the optimal areas of distribution, which at LGM were significantly lower than during the LIG and currently ($p<0.001$, Tukeys HSD multiple comparison tests) (Fig. 8).

The movements of *F. tikoua* were driven by climatic conditions. Mean temperature of the coldest month was the most important single determining factor in the LIG model, while mean temperature of the driest quarter made the largest contribution during the LGM (they contributed 27.4% and 18.4% to the LIG and LGM distribution patterns respectively, Table S1 and Table S3).

Genetic diversity of pollinator populations

Genetic diversity differs among the three regions. The YGP group had the highest COI haplotype diversity ($Hd = 0.838$) and average population SSR diversity (mean $A_R = 4.972$, mean $H_E = 0.639$), but its ITS2 genetic diversity was the lowest for both parameters. The HDM group had the highest nucleotide diversity of COI ($k = 7.017$), and highest ITS2 diversities for all parameters (Table 3). Private SSR alleles were detected in 35 populations. The highest richness of private alleles was in YQU ($P_A = 0.320$) (Table S4). The average richness of private alleles was higher in HDM and YGP than in SCB ($P_A = 0.056$, 0.063 and 0.063 for the SCB, HDM and YGP genetic groups respectively) (Table 4).

When all populations are considered, the average allele number, allele richness, expected and observed heterozygosity of SSR were 5.128 (range = 2.220 - 9.220), 4.144 (2.150 - 6.840), 0.234 (0.028 to 0.616) and 0.530 (0.276 - 0.753) respectively. The population YYS had the highest observed heterozygosity, while that at GGL had the highest allelic richness and expected heterozygosity (Table S4). Based on the genotype frequencies of SSR, significant inbreeding was present in most populations (Table S4).

The relationship between wasp clades and host floral phenotypes

Fig. 5 illustrates the association between pollinator genetic clades and the geographic distributions of male *F. tikoua* trees with either ostiolar, scattered or intermediate distributions of male flowers in their figs. Like their pollinators, host plants with different floral phenotypes had largely parapatric distributions. The geographic distributions of the different plant phenotypes loosely corresponded with the distributions of the pollinator genetic clades. Most Yungui Plateau (YGP) plants have scattered male flowers, except in the east, where most of the figs have ostiolar male flowers. Elsewhere, most figs on plants in the Hengduan Mountains (HDM) and Sichuan Basin (SCB) have ostiolar male flowers, although figs with scattered male flowers are also present in the Hengduan Mountain populations. A few host plants with apparently more than one floral phenotype (including intermediate types) were present in all three regions (Table 5). However, *F. tikoua* individuals are hard to distinguish due to their creeping life form. The different floral phenotypes recorded in the same 1 m^2 square may suggest that creeping stems of different individuals were overlapping.

From the pollinators' perspective, the host plants of SCB pollinators mostly have figs of the ostiolar type, though a few of their host figs in the contact zones have scattered and intermediate phenotypes. The host plants of YGP pollinators mostly have figs with scattered male flowers, but utilize figs with other forms in the contact zones with other pollinator groups and between two major river systems. The host plants of HDM pollinators located close to the Yangtze and Pearl river systems display a mixture of both ostiolar and scattered phenotypes, suggesting that major rivers may have blocked the expansion of *F. tikoua* populations (Fig. 5)

Fifteen of the plant populations contained male individuals that displayed the intermediate phenotype, and seven of these populations had fig wasps from two different clades breeding in their figs. This is in marked contrast to the 33 plant populations where no intermediate phenotypes were recorded, where only two populations had more than one pollinator clade present ($\text{Chi}^2{}_{[1]} = 5.099$, $p = 0.024$). Plant populations where the intermediate floral phenotype was present were also often, but not exclusively, located close to the regions where genetic barriers between pollinator clades were detected (Fig. 5). Plants with the intermediate phenotype were similarly found mostly in those populations where both scattered and ostiolar phenotypes were also present (Table 5). Non-random associations between host phenotype and pollinators' genetic structure were revealed by the chi-square tests ($\text{Chi}^2{}_{[1]} = 14.208$, $p = 0.031$ (nSSR); $\text{Chi}^2{}_{[1]} = 32.806$, $p = <0.001$ (COI)).

Discussion

Each of the three major mountain ranges that together form the Southwest China QTP sky-island complex identified by He & Jiang (2014) supports a genetically distinct group of the *Ceratosolen* sp. pollinator of *F. tikoua*. The three well defined genetic groups of the pollinator were recognized by COI and ITS2 genes, SSR genotypes and also by well-defined barriers to gene flow. Their rather limited SSR differences suggest that they are three groups within a single species, but further biological studies are necessary do determine if they should be regarded as three closely-related incipient species. The three groups have essentially parapatric geographic distributions, with little overlap, with the blue genetic clade mainly on the southeastern Yungui Plateau, the yellow clade mainly on the more western Hengduan Mountains and the northern red clade present around the Sichuan Basin.

Ancient uplift of the QTP generated the complex topography of the region, creating mountain ranges and their associated river systems, and Quaternary glacial-interglacial cycles have subsequently modified the elevations and geographical areas suitable for each plant species at different times. The complicated topography of the region will have facilitated elevational movements of species such as *F. tikoua* into refuges and also into contact zones where secondary contact between populations was possible. The distributions of the three genetic groups of *Ceratosolen* sp. pollinators loosely correspond with the distributions of the functionally significant morphological differences in the figs of their host plants, suggesting that localized co-adaptation between *Ceratosolen* sp. and its host may have taken place. For example, the morphological differences in the male figs of *F. tikoua* may be associated with varying pollination efficiency or behavior of their pollinators. Areas where their distributions do not neatly overlap may reflect the relative dispersal abilities of the plant and its pollinator, with the postglacial expansion of one pollinator genetic group failing to be matched by the spread of its associated plant phenotype, apparently because of a major river barrier.

Intra-specific differentiation of *Ceratosolen* sp. in relation to geography and history

The average K_2P distance of COI between each genetic group of the *Ceratoslen* pollinator of *F. tikoua* was 2.24%, which was about three times the average within-clade difference (0.66%). These between-clade genetic distances are smaller than those recorded between *Ceratosolen* sister species and of congeneric hymenopterous insects in general, where values of over 11.0% are typical (Hebert et al., 2003; Moe & Weiblen, 2010). The extent of COI divergence therefore indicates that *F. tikoua* is pollinated by a single species of fig wasp. This conclusion is supported by evidence that there is on-going gene flow among the three genetic groups, with combinations from different genetic groups present in 82 of the 1104 individuals for SSR genotypes. In additon, the two common ITS2 haplotypes included individuals from different COI clades which is indicative of gene exchange among the three genetic groups. Furthermore, although the three genetic groups have largely parapatric distributions, individuals from their contact zones showed considerable multiple-clade genetic components in their SSR genotypes. However, the localized spatial co-occurrence of two genetic groups (identified by their SSR genotypes) suggests the possibility that assortative mating may be taking place.

There was little overlap between the geographic distributions of the three genetic groups. The blue genetic clade occurs mainly on the southeastern Yungui Plateau, the yellow clade mainly on the more western Hengduan Mountains and the northern red clade around the Sichuan Basin. The COI sequence data showed that the blue pollinator clade diverged from the others about 5.01 Ma ago, and that the later separation of the red and yellow clades took place about 3.53 Ma ago. These estimates suggest that the three genetic groups of pollinators diverged during the Pliocene. The timing of divergence of the Yungui Pleateau (blue) group can be related to the uplift of the eastern edge of the QTP, which happened during the late Miocene and early Pliocene (Sun et al. 2011; Jacques et al. 2014; Renner 2016). The middle Pliocene divergence between the Hengduan Mountains (yellow) and Sichuan Basin (red) groups also coincides with the period of active mountain building of the Hengduan Mountains during the Miocene and Pliocene (Kirby et al., 2002; Liu et al., 2006; Sun et al., 2011). Strong dispersal barriers revealed by SSR genotypes were detected between pollinators from the Hengduan Mountains and those from the Sichuan Basin and Yungui Plateau, with a weaker barrier to gene flow between the Sichuan Basin and Yungui Plateau pollinators (Fig 4). Geographic barriers to gene flow were evidently created initially during the period of uplift.

Since their divergence, the three pollinator groups have experienced at least seven glacial and inter-glacial cycles (Augustin et al., 2004). Most recently, there were major advances by glaciers on the Tibetan Plateau during the LGM between about 45 and 25 ka ago, and glaciers will have also developed on the adjacent SW Chinese mountains where *F. tikoua* occurs today (Owen et al., 2002). Our simulations of climatic conditions during this latest glacial period indicate how the distribution of *F. tikoua* is likely to have changed during this glaciation and give an idea of how its distribution is likely to have responded to earlier glaciations.

The barriers to gene flow that mark the boundaries of the current parapatric distributions of the three pollinator genetic groups are centred on three LIG areas of suitability for their host plant. These areas were located at higher elevations than during the LGM and currently. This raises the possibility that the three genetic groups of *Ceratosolen* sp. may have diverged while they were isolated on these ‘sky islands’ during an earlier interglacial that had similar temperatures to the LIG. LIG ‘distribution bridges’ connected the Hengduan Mountains and the mountains around the Sichuan Basin, but the Yungui Plateau area was more isolated at that time. The pollinators associated with the Yungui Plateau plants (the blue clade) were the first to diverge from the others, a likely reflection of more persistent isolation resulting from their geographical location.

The inter-dependent nature of the relationship between fig trees and their pollinators means that expansions and contractions in the plant’s distribution would have resulted in parallel changes in the distributions of the insects. During the LGM, the overall area of suitable habitat in and around the Sichuan Basin increased, while the suitable habitat in the Hengduan Mountains and Yungui Plateau contracted considerably. Its typical star-like network, significant negative *Fu’s Fs*, and mismatch distribution analysis all suggest significant expansion of the red clade fig wasps that occupy the Sichuan Basin (Rogers & Harpending, 1992; Rogers, 1995; Fu, 1997; Funk & Omland, 2003; Excoffier, 2004). This recent expansion was further verified by the insects in this area having the lowest number of SSR private alleles. The Yungui Plateau (blue clade) fig wasps have also undergone significant expansion towards the end of the last glacial period. Expansions in ranges concurrent with LGM are unusual (Zhang et al., 2010; Qiu et al., 2011; Qi et al., 2012), but have been reported for *Taxus wallichiana* (Liu et al., 2013), *Osteomeles schwerinae* (Wang et al., 2015b) and *Grapholita molesta* (Song et al., 2018) in this area. The Hengduan Mountains retained very few suitable habitats for *F. tikoua* during the LGM. Reflecting this, no expansion was detected in the fig wasps from this area (the yellow clade) despite *Fu's Fs* being very sensitive indicators of expansion (Funk & Omland, 2003).

In the 'sky island' landscape, glacial cycles have increased and decreased the ranges of *F. tikoua* and its associated insects, periodically fragmenting their populations and bringing them together. Any periods of temporary contact were clearly insufficient to allow re-amalgamation of the pollinators into a single genetic group. Competition between pollinator clades and the relatively poor dispersal ability of these insects (as shown by their population structuring by distance) may have contributed to this, and there is also the possibility that the clades possess adaptations to local conditions that favor them within their core areas of distribution, including possible co-adaptations with their local host plants. Expansions and contractions of distributions in a 'sky island' terrestrial landscape make contacts between populations more dynamic than in marine archipelagoes, where the limits to distributions remain fixed over long time scales and distances between islands can be far greater. These factors can result in more limited gene flow over extended periods and more readily promote speciation and adaptations to local conditions (Bain et al., 2016).

An increasing number of fig tree species are known to be pollinated by two or more species of fig wasps, a feature that contrasts with the other well known nursery pollination system involving Yucca moths and their Yucca hosts (Smith et al., 2009; Yang et al., 2015; Yu et al., 2019b). Fig wasp colonization events followed by host switches have been reported among *Ficus* species (Wachi et al., 2016), but the northern, montane distribution of *F. tikoua* means that there is little range overlap with other *Ficus* species and fewer opportunities for host switching than would be the case for a tropical species. It is more common for fig wasps that share a host *Ficus* to be 'cryptic' species that are difficult to tell apart morphologically (Rodriguez et al., 2017; Chen et al., 2012; Darwell et al., 2014, 2017; Wachi et al., 2016; Wang et al., 2016; Segar et al., 2017; Yu et al., 2019b). They are typically sister species that have diverged during the history of their association with the plant (Yang et al., 2015; Wang et al., 2016; Souto-Vilaros et al., 2018; Yu et al., 2019b). *F. tikoua* appears to be typical in this regard, except that the extent of divergence of its pollinators has been more limited. This is despite the complex topographic environment occupied by the pollinators, and the evidence for limited dispersal by this insect (Chen et al., 2011).

Divergence within *Ceratosolen* sp. is estimated as being from 5.01 Ma, which is earlier than that of the complex of pollinator species associated with *F. septica* in Taiwan (1.9-2.0 Ma). However, caution is required regarding ages and that any dates are very tentative. Despite this a maximum difference of only 2.24% has accumulated in the pollinators of *F. tikoua*, compared with nucleotide differences of 7.2-7.8% in the pollinators of *F. septica* (Lin et al., 2008; Rodriguez et al., 2017). The deep divergence with less accumulation of variation suggests that large effective population sizes have persisted in *Ceratosolen* sp., which may reflect the high densities that *F. tikoua* populations can achieve. Furthermore, the gradual uplift of the QTP (Renner et al., 2016) appears to have only restricted, rather than eliminated, genetic exchange and may have facilitated genetic exchange between different groups at different times. We nonetheless found significant genetic differentiation and structure within *Ceratosolen* sp., some of which is linked to significant morphological variation in its host plant. Distributional responses of *F. tikoua* to future climate change are likely to determine whether the current levels of differentiation within its pollinator are maintained or increase further.

Development of the mutualism

The behavior of the pollinators of each species of dioecious fig tree can normally be identified on the basis of the floral ratios present within the figs of male individuals, because actively-pollinated species have a much lower proportion of male flowers than species that depend on passive pollination (Kjellberg et al., 2001). *Ficus tikoua* is the only recorded species where floral ratios linked to both active and passive pollination are present in different geographical areas (Deng et al., 2016). This difference is present despite their pollinators consistently exhibiting active pollen collection behavior throughout the range of the plant (Deng et al., 2016). The distributions of the three genetic groups of *Ceratosolen* sp. loosely correspond with the distributions of the functionally significant morphological differences in the figs of their host plants. The morphological differences in host inflorescences have evolved in association with genetically distinct groups of pollinators, which suggests that there may be intraspecific differences in pollinator behavior or physiology in different parts of the host's range and that intra-specific co-adaptation has taken place. Alternatively, environmental factors in part of its range may have favored the production of more male flowers to ensure adequate pollination, without co-evolved changes in the pollinator.

The intermediate inflorescence phenotype was relatively uncommon and mainly found in populations that were being pollinated by representatives of pairs of the fig wasp genetic groups rather than one group. Intermediate phenotypes were rare in populations with a combination of red and yellow genetic group pollinators present, where both genetic groups are mainly associated with the ostiolar floral phenotype elsewhere. Conversely, six of the seven plant populations containing some intermediate individuals and a pair of pollinator species had combinations of one pollinator genetic group mainly associated with ostiolar male flowers and one group mainly associated with scattered male flowers.

The concordance between pollinator genetic groups and host plant phenotypes breaks down in two areas. These are located at the western edge of the range, where there are high mountain ranges, and the South East corner of the range in an area between two major river systems. In the western area, the ranges of the plants with scattered and ostiolar male flower distributions appear to have been constrained by river systems that did not restrain the expansion of yellow clade pollinators. In the South East there is an overlap in distributions of the different male flower types in an area bordered by two major river systems where blue clade pollinators dominate. These disparities suggest that mountain ranges can be effective dispersal barriers for pollinators, with major rivers also acting as barriers to dispersal of *F. tikoua*.

Species diversification in southwest China

The sky-islands of southwest China support exceptional levels of plant diversity (He & Jiang, 2014). The topographic diversity of the region, with its associated environmental heterogeneity, facilitates this diversity, but the climatic history of the region has also contributed. Geographic barriers, in combination with climate fluctuations that fragment and re-integrate populations, can promote differentiation, but extreme fluctuations in climate also generate extinctions. The high biodiversity of the sky-islands reflects a situation where over a long period of time climate changes have tilted the balance towards speciation over extinction. There are parallels with the Cape Floral Kingdom of South Africa, where mountainous terrain, strong environmental gradients and a long period of relative climate stability have similarly combined to generate exceptional plant diversity at temperate latitudes (Simmons & Cowling, 1996; Schnitzler et al., 2011). As the situation with *F. tikoua* shows, this diversity can extend to intraspecific variation in both the plants and their associated pollinators.

Conclusions

The Quaternary ice ages have had major impacts on both tropical and temperate organisms, redistributing species and causing extinctions, fragmenting and re-joining populations and generating opportunities for divergence and speciation (Pinheiro et al., 2011; Batalha-Filho et al., 2012; Liu et al., 2013; Wang et al., 2015b, Yu et al., 2019a).

In mountainous areas, where orogenesis creates barriers to dispersal, the impacts of quaternary climate changes are complex, with varying outcomes for different taxa (Yu et al., 2019a). In the case of the 'sky islands' of SW China, their complex topography and range of elevations has clearly favored survival, differentiation and speciation over extinction, and resulted in an area of exceptional species richness. Intra-specific variation has also been facilitated and provides insights into when and where divergence between populations has occurred. The co-dependence of fig trees and their host specific pollinators allows comparisons of the responses to climate changes of organisms with widely different generation times, but closely tied geographical distributions. In the case of *F. tikoua* and its *Ceratosolen* pollinator, their three core areas of distribution in SW China have changed slightly in location in response to tectonic activities and Quaternary climate change, and the pollinators located in the three areas have diverged, but probably not to the point of being reproductively isolated. Changes have taken place in plant characters linked to pollination that partially overlap with the distributions of different pollinator groups within a single species of pollinator, which suggests that localized co-adaptation may have taken place, but evidence of adaptive changes among the pollinators is currently lacking. Our results emphasize the significance of intraspecific variation among the plants and insects of SW China's 'sky islands', which is likely to be widespread, and informative.

The long history of association between fig trees and their pollinators dates back at least several tens of millions of years, and the fundamentals of their relationship appear to have remained essentially unchanged for much of this period (Compton et al., 2010).

Speciation among the plants has generated at least 800 currently extant species, and a rather larger number of their (generally) host specific pollinators. This difference in numbers of species results largely from widely distributed fig trees being associated with different species of pollinators in different parts of their ranges. Genetic studies have shown that the pollinators that share a host in different parts of its range are usually sister species, and therefore that divergence among pollinators associated with a single species of fig tree occurs more readily among the insects than their hosts. Potential sources of isolation that allow pollinators on the same host to diverge are clear when plants are distributed across different islands (Bain et al., 2016; Rodriguez et al., 2017), but pollinators have also speciated across the ranges of continental host trees, sometimes without obvious geographical barriers to explain their current distributions (Yu et al., 2019b). The interplay between topography and climate change seen in *F. tikoua* and the 'sky islands' of SW China provides pointers to scenarios that may have led to pollinator divergence in other fig tree-fig wasp associations. The extent to which such sister species are true ecological analogues that provide identical services to their hosts, and the extent to which there is local co-adaptation, remain major unanswered questions.

Acknowledgements

We would like to express our appreciation to Lu Tan, Li-Dan Zhang, Xing Xin, Yi-Fan Li, Yi Quan, Dai-Mei Hu for their help in sample collection, Xiang Liu for suggestions on statistics, Chen-Yu Huang for extraction of bioclimatic data from

ArcGIS, Qian Zhang for advice on phylogenetic trees, Michael Cunningham for helping with species distribution models and Jaco M Greeff for suggestions with the manuscript. We would also like to thank the referees for their constructive comments. This study was supported by the National Natural Science Foundation of China (31770254, 31270387), Sichuan Science and Technology Program (2017JY0046).

References

Achimon, F., Johnson, L. A., Cocucci, A. A., Sersic, A. N., & Baranzelli, M. C. (2018). Species tree phylogeny, character evolution, and biogeography of the Patagonian genus *Anarthrophyllum* Benth. (Fabaceae). *Organisms Diversity & Evolution, 18*(1), 71-86.

Ahmed, S., Compton, S. G., Butlin, R. K., & Gilmartin, P. M. (2009). Wind-borne insects mediate directional pollen transfer between desert fig trees 160 kilometers apart. *Proceedings of the National Academy of Sciences*, *106*(48), 20342-20347.

Augustin, L., Barbante, C., Barnes, P. R., Barnola, J. M., Bigler, M., Castellano, E., … Zucchelli, M. (2004). Eight glacial cycles from an Antarctic ice core. *Nature, 429*, 623-628.

Avise, J. (2000). *Phylogeography: the history and formation of species* MA: Harvard University Press, Cambridge.

Bain, A., Borges, R., Chevallier, M. H., Vignes, H., Kobmoo, N., … Hossaert-Mckey, M. (2016). Geographic structuring into vicariant species-pairs in a wide-ranging, high-dispersal plant–insect mutualism: the case of *Ficus racemosa* and its pollinating wasps. *Evolutionary Ecology 30* (4), 663-684.

Barthlott, W., Mutke, J., Rafiqpoor, D., Kier, G., & Kreft, H. (2005). Global Centers of Vascular Plant Diversity. *Nova Acta Leopoldina NF*, *92*(342), 61-83.

Batalha-Filho, H., Cabanne, G. S., & Miyaki, C. Y. (2012). Phylogeography of an Atlantic forest passerine reveals demographic stability through the last glacial maximum. *Molecular Phylogenetics and Evolution*, *65*(3), 892-902.

Bouckaert, R., Heled, J., Kühnert, D., Vaughan, T., Wu, C. H., Xie, D., … Drummond, A. J. (2014). BEAST 2: a software platform for Bayesian evolutionary analysis. *PLoS Computational Biology*, *10*(4), e1003537.

Chen, Y., Compton, S. G., Liu, M., & Chen, X. Y. (2012). Fig trees at the northern limit of their range: the distributions of cryptic pollinators indicate multiple glacial refugia. *Molecular Ecology*, *21*(7), 1687-1701.

Chen, Y., Jiang, Z., Compton, S. G., Liu, M., & Chen, X. Y. (2011). Genetic diversity and differentiation of the extremely dwarf *Ficus tikoua* in Southwestern China.

Biochemical Systematics and Ecology, *39*(4-6), 441-448.

Cheng, R., Jiang, N., Yang, X. S., Xue, D. Y., Liu, S. X., Han, H. X. (2016). The influence of geological movements on the population differentiation of *Biston panterinaria* (Lepidoptera: Geometridae). *Journal of Biogeography*, *43*(4), 691-702.

Clement, M., Posada, D., & Crandall, K. A. (2000). TCS: a computer program to estimate gene genealogies. *Molecular Ecology*, *9*(10), 1657-1659.

Collins, W. D., Bitz, C. M., Blackmon, M. L., Bonan, G. B., Bretherton, C. S., Carton, J. A., … Kiehl, J. T. (2006). The community climate system model version 3 (CCSM3). *Journal of Climate*, *19*(11), 2122-2143.

Compton, S. G, Ball, A. D, Collinson, M. E., Hayes, P., Rasnitsyn, A. P., Ross, A. (2010). Ancient fig wasps indicate at least 34 Myr of stasis in their mutualism with fig trees. *Biology Letters*, *6* (6), 838-842.

Compton, S. G., Ellwood, M. D. F., Davis, A. J., & Welch, K. (2000). The flight heights of chalcid wasps (Hymenoptera: Chalcidoidea) in a lowland Bornean rainforest: fig wasps are the high fliers. *Biotropica*, *32*(2), 515-522.

Compton, S. G., Holton, K. C., Rashbrook, V. K., van Noort, S., Vincent, S. L., & Ware, A. B. (1991). Studies of *Ceratosolen galili*, a non-pollinating agaonid fig wasp. *Biotropica*, *23*(2)*,* 188-194.

Cornuet, J. M., Pudlo, P., Veyssier, J., Dehne-Garcia, A., Gautier, M., Leblois, R., … Estoup, A. (2014). DIYABC v2.0: a software to make approximate Bayesian computation inferences about population history using single nucleotide polymorphism, DNA sequence and microsatellite data. *Bioinformatics*, *30*(8), 1187-1189.

Cruaud, A., Rønsted, N., Chantarasuwan, B., Chou, L. S., Clement, W. L., Couloux, A., … Savolainen, V. (2012) An extreme case of plant–insect codiversification: figs and fig-pollinating wasps. *Systematic Biology*, *61*(6), 1029-1047.

Darriba, D., Taboada, G. L., Doallo, R., & Posada, D. (2012). jModelTest 2: more models, new heuristics and parallel computing. *Nature Methods*, *9*(8), 772.

Darwell, C. T., Al-Beidh, S., & Cook, J. M. (2014). Molecular species delimitation of a symbiotic fig-pollinating wasp species complex reveals extreme deviation from reciprocal partner specificity. *BMC Evolutionary Biology*, *14*(1), 189.

Darwell, C. T., & Cook, J. M. (2017). Cryptic diversity in a fig wasp community-morphologically differentiated species are sympatric but cryptic species exhibit competitive exclusion. *Molecular Ecology*, *26*(3), 937-950.

Davis, M. B., & Shaw, R. G. (2001). Range shifts and adaptive responses to Quaternary climate change. *Science*, *292*(5517), 673-679.

Deng, J. Y., Fu, R. H., Compton, S. G., Hu, D. M., Zhang, L. S., Yang, F., … Kjellberg, F. (2016) Extremely high proportions of male flowers and geographic variation in floral ratios within male figs of *Ficus tikoua* despite pollinators displaying active pollen collection. *Ecology and Evolution, 6*(2), 607-619.

Dieringer, D., & Schlötterer, C. (2003). Microsatellite analyser (MSA): a platform independent analysis tool for large microsatellite data sets. *Molecular Ecology Notes*, *3*(1), 167-169.

Earl, D. A., & vonHoldt, B. M. (2012). STRUCTURE HARVESTER: a website and program for visualizing STRUCTURE output and implementing the Evanno method. *Conservation Genetics Resources*, *4*(2), 359-361.

Evanno, G., Regnaut, S., & Goudet, J. (2005). Detecting the number of clusters of individuals using the software STRUCTURE: a simulation study. *Molecular Ecology*, *14*(8), 2611-2620.

Excoffier, L. (2004). Patterns of DNA sequence diversity and genetic structure after a range expansion: lessons from the infinite ‐ island model. *Molecular Ecology*, *13*(4), 853-864.

Excoffier, L., & Lischer, H. E. (2010). Arlequin suite ver 3.5: a new series of programs to perform population genetics analyses under Linux and Windows. *Molecular Ecology Resources*, *10*(3), 564-567.

Fan, Z. X., Liu, S. Y., Liu, Y., Liao, L. H., Zhang, X. Y., & Yue, B. S. (2012). Phylogeography of the South China field mouse (*Apodemus draco*) on the Southeastern Tibetan Plateau reveals high genetic diversity and glacial refugia. *PLoS One*, *7*(5), e38184.

Favre, A., Päckert, M., Pauls, S. U., Jähnig, S. C., Uhl, D., Michalak, I., & Muellner-Riehl, A. N. (2015). The role of the uplift of the Qinghai-Tibetan Plateau for the evolution of Tibetan biotas. *Biological Reviews*, *90*(1), 236-253.

Folmer, O., Black, M., Hoeh, W., Lutz, R., & Vrijenhoek, R. (1994). DNA primers for amplification of mitochondrial cytochrome c oxidase subunit I from diverse metazoan invertebrates. *Molecular Marine Biology and Biotechnology*, *3*(5), 294-299.

Fu, Y. X. (1997). Statistical tests of neutrality of mutations against population growth, hitchhiking and background selection. *Genetics*, *147*(2), 915-925.

Funk, D. J., & Omland, K. E. (2003). Species-level paraphyly and polyphyly: frequency, causes, and consequences, with insights from animal mitochondrial DNA. *Annual Review of Ecology, Evolution, and Systematics*, *34*(1), 397-423.

Goudet, J. (2001). FSTAT, a program to estimate and test gene diversity and fixation indices (version 2.9. 3). *http://www2. unil. ch/popgen/softwares/fstat. htm*.

Grytnes, J. A., & Mccain, C. M. (2007). Elevational trends in biodiversity. *Encyclopedia of Biodiversity*, *2*, 1-8.

Haubrich, K., & Schmitt, T. (2007). Cryptic differentiation in alpine-endemic, high-altitude butterflies reveals down-slope glacial refugia. *Molecular Ecology*, *16*(17), 3643-3658.

He, K., & Jiang, X. L. (2014). Sky islands of southwest China. I: an overview of phylogeographic patterns. *Chinese Science Bulletin*, *59*(7), 585-597.

Heald, W. F. (1951). Sky islands of Arizona. *Natural History, 60*, 95-96.

Hebert, P. D., Ratnasingham, S., & de Waard, J. R. (2003). Barcoding animal life: cytochrome c oxidase subunit 1 divergences among closely related species. *Proceedings of the Royal Society of London B: Biological Sciences*, *270*(suppl 1), S96-S99.

Herre, E. A., Jandér, K. C., & Machado, C. A. (2008). Evolutionary ecology of figs and their associates: recent progress and outstanding puzzles. *Annual Review of Ecology, Evolution, and Systematics*, *39*, 439-458.

Hewitt, G. (2000). The genetic legacy of the Quaternary ice ages. *Nature*, *405*(6789), 907.

Hewitt, G. (2004). Genetic consequences of climatic oscillations in the Quaternary. *Philosophical Transactions of the Royal Society of London B: Biological Sciences*, *359*(1442), 183-195.

Ibrahim, K. M., Nichols, R. A., & Hewitt, G. M. (1996). Spatial patterns of genetic variation generated by different forms of dispersal during range expansion. *Heredity*, *77*(3), 282-291.

Jacques, F. M., Su, T., Spicer, R. A., Xing, Y. W., Huang, Y. J., & Zhou, Z. K. (2014). Late Miocene southwestern Chinese floristic diversity shaped by the southeastern uplift of the Tibetan Plateau. *Palaeogeography, Palaeoclimatology, Palaeoecology*, *411*, 208-215.

Jevanandam, N., Goh, A. G., & Corlett, R. T. (2013). Climate warming and the potential extinction of fig wasps, the obligate pollinators of figs. *Biology Letters*, *9*(3), 20130041.

Kalinowski, S. T. (2005). HP-RARE 1.0: a computer program for performing rarefaction on measures of allelic richness. *Molecular Ecology Notes*, *5*(1), 187-189.

Kirby, E., Reiners, P. W., Krol, M. A., Whipple, K. X., Hodges, K. V., Farley, K. A., ... Chen, Z. (2002). Late Cenozoic evolution of the eastern margin of the Tibetan Plateau: Inferences from 40Ar/39Ar and (U-Th)/He thermochronology. *Tectonics*, *21*(1), 1-20.

Kjellberg, F., Jousselin, E., Bronstein, J. L., Patel, A., Yokoyama, J., & Rasplus, J. (2001). Pollination mode in fig wasps: the predictive power of correlated traits. *Proceedings of the Royal Society of London B: Biological Sciences*, *268*(1472), 1113-1121.

Kobmoo, N., Hossaert-McKey, M., Rasplus, J., & Kjellberg, F. (2010). *Ficus racemosa* is pollinated by a single population of a single agaonid wasp species in continental South-East Asia. *Molecular Ecology*, *19*(13), 2700-2712.

Librado, P., & Rozas, J. (2009). DnaSP v5: a software for comprehensive analysis of DNA polymorphism data. *Bioinformatics*, *25*(11), 1451-1452.

Lin, R. C., Yeung, C. K. L., & Li, S. H. (2008) Drastic post-LGM expansion and lack of historical genetic structure of a subtropical fig-pollinating wasp (*Ceratosolen* sp. 1) of *Ficus septica* in Taiwan. *Molecular Ecology*, *17*(23), 5008-5022.

Liu, J., Möller, M., Provan, J., Gao, L. M., Poudel, R. C., & Li, D. Z. (2013). Geological and ecological factors drive cryptic speciation of yews in a biodiversity hotspot. *New Phytologist*, *199*(4), 1093-1108.

Liu, J. Q., Wang, Y. J., Wang, A. L., Hideaki, O., & Abbott, R. J. (2006). Radiation and diversification within the *Ligularia-Cremanthodium-Parasenecio* complex (Asteraceae) triggered by uplift of the Qinghai-Tibetan Plateau. *Molecular Phylogenetics and Evolution*, *38*(1), 31-49.

Liu, M., Zhao, R., Chen, Y., Zhang, J., Compton, S. G., & Chen, X. Y. (2014). Competitive exclusion among fig wasps achieved via entrainment of host plant flowering phenology. *PLoS One*, *9*(5), e97783.

Liu, Q., Chen, P., He, K., Kilpatrick, C. W., Liu, S. Y., Yu, F. H., & Jiang, X. L. (2012). Phylogeographic study of *Apodemus ilex* (Rodentia: Muridae) in southwest China. *PLoS One*, *7*(2), e31453.

Lomolino, M. V. (2001). Elevation gradients of species-density: historical and prospective views. *Global Ecology and Biogeography*, *10*(1), 3-13.

Lopez-Vaamonde, C., Rasplus, J. Y., Weiblen, G. D., & Cook, J. M. (2001). Molecular phylogenies of fig wasps: partial cocladogenesis of pollinators and parasites. *Molecular Phylogenetics and Evolution*, *21*(1), 55-71.

Manni, F., Guerard, E., & Heyer, E. (2004). Geographic patterns of (genetic, morphologic, linguistic) variation: how barriers can be detected by using Monmonier's algorithm. *Human Biology*, *76*(2), 173-190.

Margraf, N., Verdon, A., Rahier, M., & Naisbit, R. E. (2007). Glacial survival and local adaptation in an alpine leaf beetle. *Molecular Ecology*, *16*(11), 2333-2343.

Mayol, M., Riba, M., González-Martínez, S. C., Bagnoli, F., de Beaulieu, J., Berganzo, E., … Vendramin, G. G. (2015). Adapting through glacial cycles: insights from a long-lived tree (*Taxus baccata*). *New Phytologist*, *208*(3), 973-986.

McCormack, J. E., & Smith, T. B. (2008). Niche expansion leads to small-scale adaptive divergence along an elevation gradient in a medium-sized passerine bird. *Proceedings of the Royal Society B: Biological Sciences*, *275*(1647), 2155-2164.

McLaughlin, S. P. (1994). An overview of the flora of the Sky Islands, southeastern Arizona: diversity, affinities, and insularity. *Biodiversity and Management of the Madrean Archipelago: the Sky Islands of Southwestern United States and Northwestern Mexico*, 60-70.

Mirol, P. M., Routtu, J., Hoikkala, A. & Butlin, R. K. (2008). Signals of demographic expansion in *Drosophila virilis*. *BMC Evolutionary Biology*, *8*(1), 59.

Moe, A. M., & Weiblen, G. D. (2010). Molecular divergence in allopatric *Ceratosolen* (Agaonidae) pollinators of geographically widespread *Ficus* (Moraceae) species. *Annals of the Entomological Society of America*, *103*(6), 1025-1037.

Molbo, D., Machado, C. A., Sevenster, J. G., Keller, L., & Herre, E. A. (2003). Cryptic species of fig-pollinating wasps: implications for the evolution of the fig–wasp mutualism, sex allocation, and precision of adaptation. *Proceedings of the National Academy of Sciences*, *100*(10), 5867-5872.

Myers, N., Mittermeier, R. A., Mittermeier, C. G., Da Fonseca, G. A., & Kent, J. (2000). Biodiversity hotspots for conservation priorities. *Nature*, *403*(6772), 853-858.

Nazareno, A. G., Alzate-Marin, A. L., & Pereira, R. A. S. (2013). Dioecy, more than monoecy, affects plant spatial genetic structure: the case study of *Ficus*. *Ecology and Evolution*, *3*(10), 3495-3508.

Noroozi, J., Talebi, A., Doostmohammadi, M., Rumpf, S. B., Linder, H. P., & Schneeweiss, G. M. (2018). Hotspots within a global biodiversity hotspot - areas of endemism are associated with high mountain ranges. *Scientific Reports*, *8*(1), 10345.

Owen, L. A., Finkel, R. C., & Caffee, M. W. (2002). A note on the extent of glaciation throughout the Himalaya during the global Last Glacial Maximum. *Quaternary Science Reviews*, *21*(1-3), 147-157.

Phillips, S. J., & Dudík, M. (2008). Modeling of species distributions with Maxent: new extensions and a comprehensive evaluation. *Ecography*, *31*(2), 161-175.

Pinheiro, F., de Barros, F., Palma-Silva, C., Fay, M. F., Lexer, C., & Cozzolino, S. (2011). Phylogeography and genetic differentiation along the distributional range of the orchid *Epidendrum fulgens*: a Neotropical coastal species not restricted to glacial refugia. *Journal of Biogeography*, *38*(10), 1923-1935.

Polfus, J. L., Manseau, M., Klütsch, C. F., Simmons, D., & Wilson, P. J. (2017). Ancient diversification in glacial refugia leads to intraspecific diversity in a Holarctic mammal. *Journal of Biogeography*, *44*(2), 386-396.

Popp, M., Gizaw, A., Nemomissa, S., Suda, J. & Brochmann, C. (2008). Colonization and diversification in the African 'sky islands' by *Eurasian Lychnis* L.(Caryophyllaceae). *Journal of Biogeography*, *35*(6), 1016-1029.

Pritchard, J. K., Stephens, M., & Donnelly, P. (2000). Inference of population structure using multi-locus genotype data. *Genetics*, *155*(2), 945-959

Qi, X. S., Chen, C., Comes, H. P., Sakaguchi, S., Liu, Y. H., Tanaka, N., … Qiu, Y. X. (2012). Molecular data and ecological niche modelling reveal a highly dynamic evolutionary history of the East Asian Tertiary relict *Cercidiphyllum* (Cercidiphyllaceae). *New Phytologist*, *196*(2), 617-630.

Qiu, Y. X., Fu, C. X., & Comes, H. P. (2011). Plant molecular phylogeography in China and adjacent regions: tracing the genetic imprints of Quaternary climate and environmental change in the world's most diverse temperate flora. *Molecular Phylogenetics and Evolution*, *59*(1), 225-244.

Qu, Y. H., Luo, X., Zhang, R. Y., Song, G., Zou, F. S., & Lei, F. M. (2011). Lineage diversification and historical demography of a montane bird *Garrulax elliotii* - implications for the Pleistocene evolutionary history of the eastern Himalayas. *BMC Evolutionary Biology*, *11*(1), 174.

Rafiqpoor, D., Kier, G., & Kreft, H. (2005). Global centers of vascular plant diversity. *Nova Acta Leopoldina NF*, *92*(342), 61-83.

Rambaut, A. & Drummond, A. J. (2009). Tracer v1.5. http://beast.bio.ed.ac.uk/Tracer.

Renner, S. S. (2016). Available data point to a 4-km-high Tibetan Plateau by 40 Ma, but 100 molecular-clock papers have linked supposed recent uplift to young node ages. *Journal of Biogeography*, *43*(8), 1479-1487.

Rodriguez, L. J., Bain, A., Chou, L. S., Conchou, L., Cruaud, A., Gonzales, R., ... Kjellberg, F. (2017). Diversification and spatial structuring in the mutualism between Ficus septica and its pollinating wasps in insular South East Asia. *BMC Evolutionary Biology*, *17*(1),1-12.

Rogers, A. R. (1995). Genetic evidence for a Pleistocene population explosion. *Evolution*, *49*(4), 608-615.

Rogers, A. R. & Harpending, H. (1992). Population growth makes waves in the distribution of pairwise genetic differences. *Molecular Biology and Evolution*, *9*(3), 552-569.

Ronquist, F., Teslenko, M., Van Der Mark, P., Ayres, D. L., Darling, A., Höhna, S., … Huelsenbeck, J. P. (2012). MrBayes 3.2: efficient Bayesian phylogenetic inference and model choice across a large model space. *Systematic Biology*, *61*(3), 539-542.

Rousset, F. (2008). GENEPOP'007: a complete re-implementation of the GENEPOP software for Windows and Linux. *Molecular Ecology Resources*, *8*(1), 103-106.

Sambrook, J., Fritsch, E., & Maniatis, T. (1989). *Molecular cloning: a laboratory manual* Cold Spring Harbor.

Schnitzler, J., Barraclough, T.G., Boatwright, J.S., Goldblatt, P., Manning, J.C., Powell, M.P., Rebelo, T. & Savolainen, V. (2011). Causes of plant diversification in the Cape biodiversity hotspot of South Africa. *Systematic Biology*, *60*(3), 343–357.

Segar, S. T., Volf, M., Zima Jnr, J., Isua, B., Sisol, M., Sam, L., … Novotny, V. (2017). Speciation in a keystone plant genus is driven by elevation: a case study in New Guinean *Ficus*. *Journal of Evolutionary Biology*, *30*(3), 512-523.

Sharma, A., Poudel, R. C., Li, A., Xu, J. C., & Guan, K. Y. (2014). Genetic diversity of *Rhododendron delavayi* var. *delavayi* (CB Clarke) Ridley inferred from nuclear and chloroplast DNA: implications for the conservation of fragmented populations. *Plant Systematics and Evolution*, *300*(8), 1853-1866.

Simmons, M. T. & Cowling, R. M. (1996). Why is the Cape Peninsula so rich in plant species? An analysis of the independent diversity components. *Biodiversity and Conservation*, *5*(5), 551-573.

Smith, C. I., Drummond, C. S., Godsoe, W., Yoder, J. B., & Pellmyr, O. (2009). Host specificity and reproductive success of yucca moths (*Tegeticula* spp. Lepidoptera: Prodoxidae) mirror patterns of gene flow between host plant varieties of the Joshua tree (*Yucca brevifolia*: Agavaceae). *Molecular Ecology*, *18*(24), 5218-5229.

Song, W., Cao, L. J., Li, B. Y., Gong, Y. J., Hoffmann, A. A., & Wei, S. J. (2018). Multiple refugia from penultimate glaciations in East Asia demonstrated by phylogeography and ecological modelling of an insect pest. *BMC Evolutionary Biology*, *18*(1), 152.

Souto-Vilaros, D., Proffit, M., Buatois, B., Rindos, M., Sisol, M., Kuyaiva, T., … Segar, S. T. (2018). Pollination along an elevational gradient mediated both by floral scent and pollinator compatibility in the fig and fig-wasp mutualism. *Journal of Ecology*, *106*(6), 2256-2273.

Sun, B. N., Wu, J. Y., Liu, Y. S., Ding, S. T., Li, X. C., Xie, S. P., ... Lin, Z. C. (2011). Reconstructing Neogene vegetation and climates to infer tectonic uplift in western Yunnan, China. *Palaeogeography, Palaeoclimatology, Palaeoecology*, *304*(3-4), 328-336.

Swofford, D. (2002). *PAUP*. Phylogenetic analysis using parsimony (and other methods), 4.0 beta.* Smithsonian Institution, Washington DC, Sinauer, Sunderland, MA.

Tajima, F., (1989). The effect of change in population size on DNA polymorphism. *Genetics*, *123*(3), 597-601.

Tamura, K., Peterson, D., Peterson, N., Stecher, G., Nei, M., & Kumar, S. (2011). MEGA5: molecular evolutionary genetics analysis using maximum likelihood, evolutionary distance, and maximum parsimony methods. *Molecular Biology and Evolution*, *28*(10), 2731-2739.

Tan, L., Deng, J. Y., Fu, R. H., & Chen, Y. (2016). Isolation and characterization of 13 polymorphic microsatellite loci for the fig wasp, *Ceratosolen sp.*(Hymenoptera: Agaonidae). *Applied Entomology and Zoology*, *51*(2), 317-320.

Valdeyron, G., & Lloyd, D. G. (1979). Sex differences and flowering phenology in the common fig, *Ficus carica* L. *Evolution*, *33*(2), 673-685.

Wachi, N., Kusumi, J., Tzeng, H. Y., & Su, Z. H. (2016). Genome-wide sequence data suggest the possibility of pollinator sharing by host shift in dioecious figs (Moraceae, *Ficus*). *Molecular Ecology*, *25*(22), 5732-5746.

Wang, G., Cannon, C. H., & Chen, J. (2016). Pollinator sharing and gene flow among closely related sympatric dioecious fig taxa. *Proceedings: Biological Sciences*, *283*(1828), 20152963.

Wang, R., Compton, S. G., Quinnell, R. J., Peng, Y. Q., Barwell, L., & Chen, Y. (2015a). Insect responses to host plant provision beyond natural boundaries: latitudinal and altitudinal variation in a Chinese fig wasp community. *Ecology and Evolution*, *5*(17), 3642-3656.

Wang, Z. W., Chen, S. T., Nie, Z. L., Zhang, J. W., Zhou, Z., Deng, T., & Sun, H. (2015b). Climatic factors drive population divergence and demography: insights based on the phylogeography of a riparian plant species endemic to the Hengduan Mountains and adjacent regions. *PLoS One*, *10*(12), e0145014.

Ware, A. B., & Compton, S. G. (1994). Dispersal of adult female fig wasps: 2. Movements between trees. *Entomologia Experimentalis et Applicata*, *73*(3), 231-238.

Willig, M. R., Kaufman, D. M., & Stevens, R. D. (2003). Latitudinal gradients of biodiversity: pattern, process, scale, and synthesis. *Annual Review of Ecology, Evolution, and Systematics*, *34*(1), 273-309.

Xu, H. G., Cao, M. C., Wu, Y., Cai, L., Cao, Y., Wu, J., … Cui, P. (2016). Disentangling the determinants of species richness of vascular plants and mammals from national to regional scales. *Scientific Reports*, *6*, 21988.

Yang, L. Y., Machado, C. A., Dang, X. D., Peng, Y. Q., Yang, D. R., Zhang, D. Y., & Liao, W. J. (2015). The incidence and pattern of copollinator diversification in dioecious and monoecious figs. *Evolution*, *69*(2), 294-304.

Yu, H. B., Deane, D. C., Sui, X. H., Fang, S. Q., Chu, C. J., Liu, Y., & He, F. L. (2019a). Testing multiple hypotheses for the high endemic plant diversity of the Tibetan Plateau. *Global Ecology and Biogeography*, *28*(2), 131-144.

Yu, H., Tian, E. W., Zheng, L. N., Deng, X. X., Cheng, Y. F., Chen, L. F., ... Compton, S. G. (2019b). Multiple parapatric pollinators have radiated across a continental fig tree displaying clinal genetic variation. *Molecular Ecology*, *28*(9), 2391-2405.

Zhang, D. R., Chen, M. Y., Murphy, R. W., Che, J., Pang, J. F., Hu, J. S., … Zhang, Y. P. (2010). Genealogy and palaeodrainage basins in Yunnan Province: phylogeography of the Yunnan spiny frog, *Nanorana yunnanensis* (Dicroglossidae). *Molecular Ecology*, *19*(16), 3406-3420.

Zhang, J. Q., Meng, S. Y., & Rao, G. Y. (2014). Phylogeography of *Rhodiola kirilowii* (Crassulaceae): a story of Miocene divergence and Quaternary expansion. *PLoS One*, *9*(11), e112923.

Zhang, Z. Y., Zheng, X. M., & Ge, S. (2007). Population genetic structure of *Vitex negundo* (Verbenaceae) in Three-Gorge Area of the Yangtze River: The riverine barrier to seed dispersal in plants. *Biochemical Systematics and Ecology*, *35*(8), 506-516.

Zhao, T. T., Compton, S. G., Yang, Y. J., Wang, R., & Chen, Y. (2014). Phenological adaptations in *Ficus tikoua* exhibit convergence with unrelated extra-tropical fig trees. *PLoS ONE, 9*(12), e114344.

Zheng, W. J., Fu, G. L., & Zhao, Q. S. (1978). Flora reipublicae popularis sinicae, Tomus 7. Science Press, Beijing, China.

Zhou, Y. D., Chen, S. C., Hu, G. W., Mwachala, G., Yan, X., Wang, Q. F. (2018). Species richness and phylogenetic diversity of seed plants across vegetation zones of Mount

Kenya, East Africa. *Ecology and Evolution*, *8*(17), 8930-8939

Author Contributions

Y. Chen designed the study. J.Y. Deng, R.H. Fu, M. Liu, Q. Wang, C. Yuan and L.S. Zhang collected the samples, processed the samples and analyzed the data. J. Y. Deng, R. H. Fu, S. G. Compton and Y. Chen interpreted the data and wrote the manuscript.

Data Accessibility:

DNA sequences of COI haplotypes: GenBank accessions MK241697-241765.
DNA sequences of ITS2 haplotypes: GenBank accessions MK241766-241783.
Sampling location, bioclimate data, MaxEnt input files, final assembly of COI, ITS2 and microsatellite genotypes of wasp individuals and the distribution patterns of male flower of *Ficus tikoua* are archived in the Dryad Digital Repository at http://datadryad.org, doi: 10.5061/dryad.xpnvx0kb5.

Figure Legends:

Fig. 1 The distribution of *Ficus tikoua* in SW China, based on the Chinese Virtual Herbarium (CVH), the Global Biodiversity Information Facility (GBIF) (green dots) and our own records (purple dots).

Fig. 2 Flow chart illustrating batched analysis steps. Detailed information is provided in the main text.

Fig. 3 The Bayesian tree (left) and network (right) of COI sequences of *Ceratosolen* sp. pollinators of *Ficus tikoua*. Posterior probabilities of above 0.5 are shown under the branches, and simulated node ages are shown on the branches. Three monophyletic clades are highlighted in red, yellow and blue. In the network, each haplotype is indicated by an ellipse with their frequencies indicated by the sizes of each ellipse. The colors are concordant with those of the corresponded clades in the Bayesian tree.

Fig. 4 The microsatellite memberships of *Ceratosolen* sp. individuals assigned by STRUCTURE. Each vertical line represents one individual. The three colors indicate each microsatellite group. Their geographical distributions are indicated by YGP (Yungui Plateau), HDM (Hengduan Mountains) and SBC (Sichuan Basin). Gene flow barriers identified by Barrier v2 are highlighted by grey blocks. The populations were indicated by numbers, which are corresponded with the population codes in Table 1.

Fig. 5 The distributions of the three genetic groups of the *Ceratosolen* sp. associated with *Ficus tikoua* in Southwest China (red, yellow and blue circles) and their relationship to phenotypic characters of their host plants. The boundary areas reflecting barriers to gene flow, based on SSR data, are indicated by red lines. Yangtze river and Pearl river were indicated by blue lines.
(a) genetic groups based on SSR substructure (K=3).
(b) genetic groups based on COI. Background shading indicates the male flower distributions in their host figs (ostiolar = purple, scattered = green). The populations with intermediate male flower distributions were indicated by yellow halos around the population circles. Note that intermediate male flower distributions are more frequently present in populations where pollinators from pairs of COI genetic groups are present.

Fig. 6 A Bayesian skyline plot of past population demographic trends of gene COI in three genetic clades of *Ceratosolen* sp. pollinators of *Ficus tikoua*. Red, yellow and blue clades are represented by lines in their corresponding colors. Colored dashed lines indicate 95% probability density intervals.

Fig. 7 Distributions of *Ficus tikoua* simulated by ecological niche models using bioclimatic variables. (a) LIG (last interglacial); (b) LGM (last global maximum); (c) Current distribution. Red lines indicate gene flow barriers based on SSR data.

Fig. 8 Boxplots of elevation, longitude and latitude of *Ficus tikoua* populations at different times (LIG, LGM, Current). Means and standard deviations (SD) are indicated by red dots and arrows respectively.

Tables

Table 1 Sampled populations of *Ceratosolen* fig wasps and their genetic compositions in Southwest China. N_{SSR}, N_{COI}, and N_{ITS} indicate the numbers of individuals used in microsatellite genotype scanning (SSR), and COI and ITS2 gene sequencing, respectively. The COI and ITS2 haplotypes present in each population are listed as C01-C69, and I01-I18 respectively. The numbers in parentheses indicate the number of individuals with each haplotype copy.

Code No.	Code	Population	Latitude (°N)	Longitude (°E)	Altitude (m)	Sample sizes				Haplotypes (Copies)	
						N_{fig}	N_{SSR}	N_{COI}	N_{ITS}	COI	ITS2
1	YMJ	Mingjiu	23.42	103.75	1836.69	17	27	10	10	C10 (6), C19 (2), C20 (1), C21 (1)	I01 (8), I08 (2)
2	YMZ	Mengzi	23.37	103.53	1782.85	28	28	10	10	C10 (6), C24 (4)	I01 (7), I08 (3)
3	YYS	Yanshan	23.65	104.29	1589.73	16	23	10	10	C19 (5), C39 (2), C40 (2), C41 (1)	I01 (8), I12 (2)
4	GTY	Tianyang	23.95	107.10	477.24	25	29	9	10	C56 (3), C57 (3), C58 (1), C59 (2)	I01 (10)
5	GYZ	Yizhou	24.37	108.74	256.41	28	28	10	9	C46 (10)	I01 (8), I15 (1)
6	GLZ	Luzhai	24.53	109.88	123.67	18	26	9	10	C46 (9)	I01 (9), I15 (1)
7	GDL	Donglan	24.56	107.74	330.60	21	23	10	9	C46 (5), C50 (1), C51 (1), C52 (2), C53 (1)	I01 (7), I15 (2)
8	GHC	Hechi	24.57	108.46	183.08	29	29	10	10	C46 (10)	I01 (9), I15 (1)
9	GLL	Longlin	24.98	105.48	433.06	16	26	10	10	C50 (10)	I01 (10)
10	GND	Nandan	25.29	107.37	823.44	11	18	10	9	C46 (1), C50 (8), C54 (1)	I01 (9)
11	CSJ	Cong-Shanjiang	25.77	108.95	202.44	28	28	10	10	C46 (4), C50 (6)	I01 (6), I15 (4)
12	YSH	Shiping-Tonghai	23.93	102.63	1665.5	26	30	10	10	C10 (3), C24 (1), C30 (1), C31 (1), C32 (1), C34 (2), C35 (1)	I01 (9), I08 (1)
13	YJS	Jianshui	23.61	103.06	1268.57	6	17	10	9	C09 (1), C10 (8), C11 (1)	I01 (9)
14	YPZ	Puzhehei	24.09	104.05	1550.00	9	15	10	9	C10 (7), C19 (2), C29 (1)	I01 (9)
15	YLP	Luoping	25.05	104.55	1231.39	28	28	10	9	C46 (2), C50 (7), C51 (1)	I01 (8), I17 (1)
16	GGL	Guanling	25.93	105.63	847.11	29	29	10	7	C49 (1), C50 (9)	I01 (7)
17	GTL	Tianlong	26.42	106.10	1350.73	7	14	9	9	C44 (3), C45 (2), C50 (3), C53 (1)	I01 (6), I03 (3)

18	GSD	Sandu	26.06	107.87	488.86	29	29	9	10	C01 (2), C50 (5), C54 (2)	I01 (8), I03 (2)
19	YJY	Jingyan	24.22	102.57	1747.75	10	12	10	10	C12 (10)	I06 (10)
20	YLX	Luxi	24.70	103.51	1956.36	15	30	10	8	C10 (2), C14 (3), C15 (1), C16 (1), C17 (1), C18 (2)	I01 (5), I08 (3)
21	YQU	Qujing	25.54	103.71	1914.13	17	17	9	6	C14 (2), C64 (7)	I01 (4), I08 (2)
22	YXW	Xuanwei	26.22	104.06	2082.62	11	11	8	8	C14 (2), C68 (1), C69 (5)	I08 (8)
23	YKM	Kuming	25.07	102.61	2234.00	16	26	10	9	C13 (10)	I06 (5), I08 (3), I18 (1)
24	SXC	Xichang	27.87	102.28	1716.16	8	25	10	10	C13 (1), C27 (1), C28 (2), C36 (2), C37 (1), C43 (1), C60 (1), C61 (1)	I08 (1), I11 (8), I14 (1)
25	YWD	Wuding	25.54	102.39	1841.75	28	28	10	10	C13 (9), C36 (1)	I06 (4), I08 (6)
26	SPZ	Panzhihua	26.39	101.77	1276.04	27	27	10	10	C13 (5), C25 (2), C27 (2), C28 (1)	I08 (7), I10 (3)
27	YHZ	Huize	26.49	103.17	2051.07	20	20	8	7	C12 (1), C25 (5), C63 (2)	I08 (3), I10 (4)
28	YQJ	Qiaojia	26.89	102.97	1633.59	24	26	10	9	C13 (7), C25 (2), C55 (1)	I08 (3), I10 (6)
29	YLD	Ludian	27.01	103.32	1366.89	7	13	10	10	C13 (10)	I08 (8), I10 (2)
30	SYY	Yanyuan	27.24	101.86	1569.35	30	31	10	10	C13 (6), C42 (1), C43 (2), C62 (1)	I08 (5), I11 (4), I13 (1)
31	SMH	Mahu	28.45	103.80	983.41	24	24	8	7	C65 (3), C66 (5)	I08 (8)
32	SHS	Shimian	29.19	102.40	1134.43	26	26	10	10	C03 (1), C47 (8), C48 (1)	I03 (8), I16 (2)
33	SLS	Leshan	29.46	103.73	358.60	24	24	9	10	C03 (8), C67 (1)	I03 (7), I05 (3)
34	GKY	Kaiyang	27.07	107.06	970.12	7	13	8	9	C44 (7), C45 (1)	I01 (1), I03 (8)
35	SGL	Guling	28.05	105.79	585.74	9	17	10	10	C03 (5), C06 (4), C07 (1)	I03 (9), I04 (1)
36	SJA	Jiangan	28.63	105.08	342.34	27	27	10	10	C03 (9), C04 (1)	I03 (4), I04 (6)
37	SNX	Naxi	28.75	105.56	534.41	11	16	10	10	C03 (8), C26 (2)	I04 (10)
38	SYJ	Yingjing	29.68	102.85	949.74	30	30	10	10	C03 (5), C38 (5)	I03 (3), I05 (7)
39	SFY	Fengya	30.14	106.90	297.62	28	28	10	9	C01 (3), C02 (3), C03 (1), C04 (2), C05 (1)	I02 (4), I03 (3), I04 (2)
40	SSP	Shipan	30.41	106.23	286.00	26	26	10	9	C02 (4), C03 (3), C08 (2), C33 (1)	I03 (1), I04 (8)
41	SSN	Suining	30.52	105.48	324.00	27	27	10	10	C02 (6), C03 (4)	I03 (2), I04 (8)
42	SNC	Nanchong	30.78	106.08	275.00	25	25	10	10	C02 (3), C03 (4), C04 (1), C08 (2)	I03 (4), I04 (6)

43	SGJ	Guangji	31.27	104.05	683.00	22	29	10	9	C03 (10)	I03 (4), I05 (5)
44	SMY	Mianyang	31.34	104.53	516.00	28	28	11	10	C03 (5), C08 (2), C22 (2), C23 (2)	I03 (4), I04 (4), I05 (1), I07 (1), I09 (1)
45	SBZ	Bazhong	31.82	107.01	450.71	29	29	10	10	C01 (4), C02 (4), C03 (2)	I02 (2), I03 (8)
46	SCQ	Chongqing	29.39	106.40	317.69	5	8	10	9	C03 (8), C04 (2)	I03 (4), I04 (5)
47	SJY	Jianyang	30.33	104.76	389.54	6	7	10	10	C03 (9), C08 (1)	I03 (1), I04 (1), I07 (8)
48	SGY	Guangyuan	32.42	105.83	555.96	5	7	10	9	C02 (5), C08 (5)	I03 (9)

Table 2 Neutrality tests and mismatch analyses for three genetic clades, based on gene COI. *SSD*, sum of squared deviations.

					Sudden Expansion Model		Spatial Expansion Model	
Clades	Tajima's *D*	*p(D)*	Fu's *Fs*	*p(Fs)*	*SSD*	*p(SSD)*	*SSD*	*p(SSD)*
Red clade	-1.349	0.076	-7.099	0.011	0.002	0.789	0.002	0.802
Yellow clade	-1.097	0.115	-3.214	0.133	0.637	<0.001	0.021	0.593
Blue clade	0.305	0.681	-8.893	0.023	0.042	0.011	0.032	0.208

Table 3 Genetic diversities of three regions based on COI and ITS2 (shown in parentheses with italic) genes. n, number of individuals; *S*, polymorphic sites excluding gaps; *h*, number of haplotypes; *Hd*, haplotype diversities; π, nucleotide diversities; *k*, average number of nucleotide diversities; POP N., number of populations; Indv. N., number of pollinator wasps per population.

groups	Pool Data							Population Average							
	n	S	h	Hd	π	k	$\theta(\pi)$	POP N.	Indv. N.	S	h	Hd	π	k	$\theta(\pi)$
SCB	168	27	18	0.730	0.002	1.510	0.002	17	9.824	2.824	2.647	0.478	0.002	1.022	0.002
	(165)	*(7)*	*(6)*	*(0.558)*	*(0.001)*	*(0.652)*	*(0.001)*		*(9.765)*	*(1.059)*	*(1.882)*	*(0.282)*	*(0.001)*	*(0.354)*	*(0.001)*
HDM	123	34	25	0.827	0.011	7.017	0.011	13	9.3385	8.154	3.077	0.468	0.005	3.484	0.014
	(113)	*(7)*	*(5)*	*(0.580)*	*(0.002)*	*(1.124)*	*(0.002)*		*(8.846)*	*(1.308)*	*(1.692)*	*(0.318)*	*(0.001)*	*(0.658)*	*(0.001)*
YGP	176	33	30	0.838	0.008	5.293	0.008	18	9.778	5.056	2.944	0.457	0.003	1.930	0.003
	(170)	*(6)*	*(4)*	*(0.146)*	*(0.001)*	*(0.579)*	*(0.001)*		*(9.444)*	*(1.333)*	*(1.333)*	*(0.124)*	*(0.001)*	*(0.494)*	*(0.001)*

Table 4 Genetic diversities of three regions of *Ceratosolen* sp. microsatellites. (Number of individuals (N_{SSR}), number of alleles (N_A), allelic richness after rarefication (A_R), observed (H_O) and expected (H_E) heterozygosity with significance for deviation from HWE ($^{*}p < 0.05$, $^{**}p < 0.01$, $^{***}p < 0.001$) after correction for multiple testing, inbreeding coefficient (F_{IS}) ($^{*}p < 0.05$), and private allelic richness (P_A); Indv. N., number of pollinator wasps per population).

Groups	Pool Data						Population Average						
	N_{SSR}	N_A	A_R	H_O/ H_E	F_{IS}	PA	POP N.	Indv. N.	N_A	A_R	H_O/ H_E	F_{IS}	PA
SCB	345	13.556	13.21	$0.155/0.630^{***}$	0.753^{*}	1.43	14	22.308	4.618	3.704	0.153/0.463	0.696	0.056
HDM	290	13.222	13.20	$0.222/0.629^{***}$	0.663^{*}	1.33	13	24.643	4.181	3.469	0.222/0.452	0.525	0.063
YGP	447	15.222	14.82	$0.299/0.811^{***}$	0.645^{*}	3.61	18	24.833	6.209	4.972	0.305/0.639	0.534	0.063
All	1082	19.778	19.76	0.232/0.812	0.714		45	24.022	5.128	4.144	0.234/0.530	0.582	0.061

Table 5 The numbers of host plant with three different types of male flower distribution across three wasps genetic groups. N, number of populations.

Genetic Groups	N	Individuals with Scattered figs	Individuals with Intermediate figs	Individuals with Ostiolar figs	Individuals with mixed fig types	% Scattered
YGP	20	51	1	24	24	51.00
HDM	10	8	0	34	2	18.18
SCB	11	1	0	37	10	2.08

Fig. 1

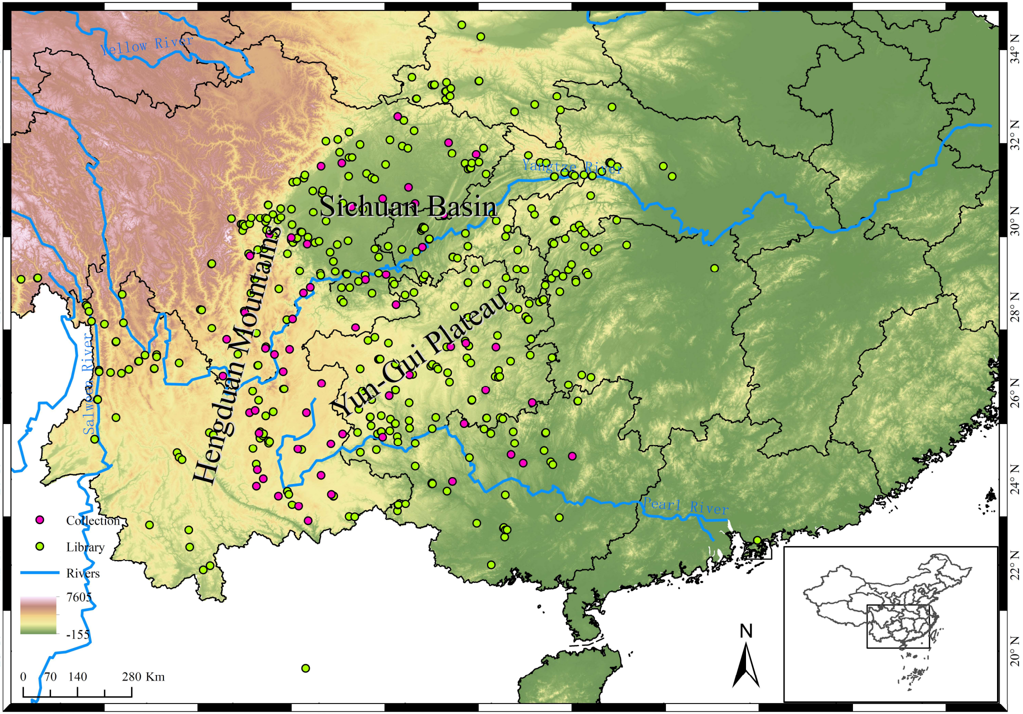
98° E
100° E
102° E
104° E
106° E
108° E
110° E
112° E
114° E
116° E
118° E
34° N
32° N
30° N
28° N
26° N
24° N
22° N
20° N
Yellow River
Yangtze River
Pearl River
Salween River
Sichuan Basin
Hengduan Mountains
Yun-Gui Plateau
● Collection
● Library
Rivers
7605
-155
0
70
140
280 Km
N

Fig. 2

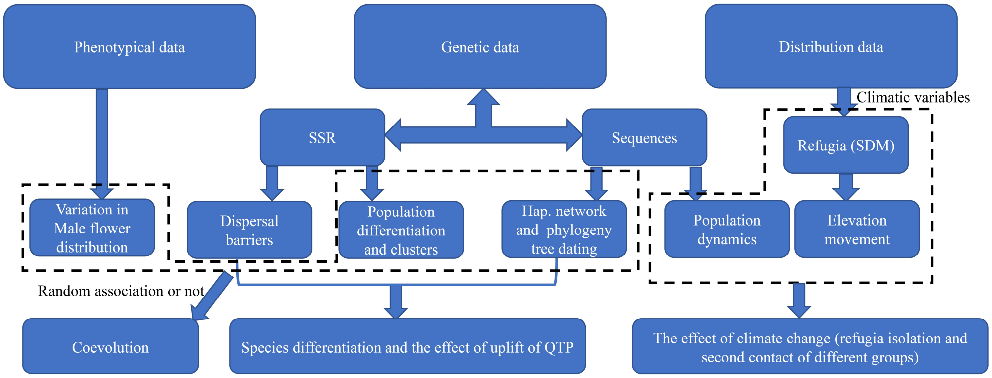
Phenotypical data
Genetic data
Distribution data
Climatic variables
SSR
Sequences
Refugia (SDM)
Variation in Male flower distribution
Dispersal barriers
Population differentiation and clusters
Hap. network and phylogeny tree dating
Population dynamics
Elevation movement
Random association or not
Coevolution
Species differentiation and the effect of uplift of QTP
The effect of climate change (refugia isolation and second contact of different groups)

Fig. 3

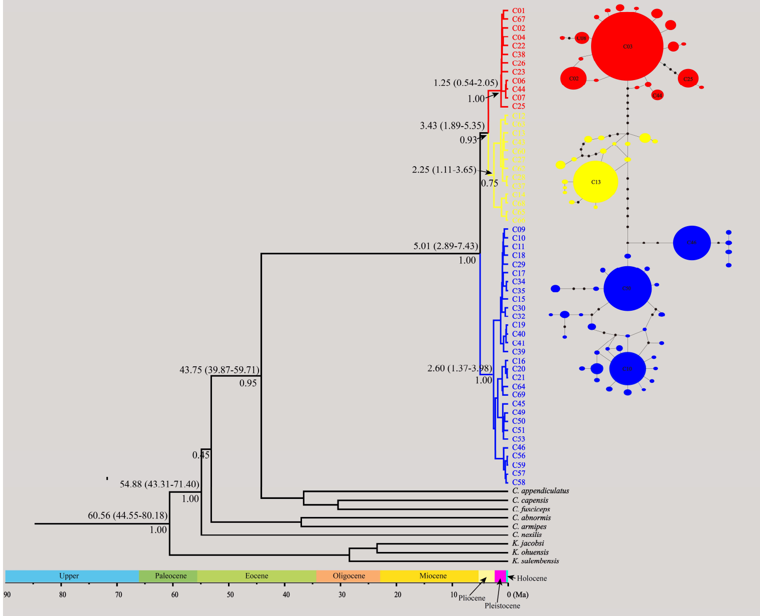

C01
C67
C02
C04
C22
C38
C26
C23
C06
C44
C07
C25
C12
C63
C13
C43
C60
C27
C62
C28
C37
C14
C68
C65
C66
C09
C10
C11
C18
C29
C17
C34
C35
C15
C30
C32
C19
C40
C41
C39
C16
C20
C21
C64
C69
C45
C49
C50
C51
C53
C46
C56
C59
C57
C58
C. appendiculatus
C. capensis
C. fusciceps
C. abnormis
C. armipes
C. nexilis
K. jacobsi
K. ohuensis
K. salembensis
1.25 (0.54-2.05)
1.00
3.43 (1.89-5.35)
0.93
2.25 (1.11-3.65)
0.75
5.01 (2.89-7.43)
1.00
2.60 (1.37-3.98)
1.00
43.75 (39.87-59.71)
0.95
0.45
54.88 (43.31-71.40)
1.00
60.56 (44.55-80.18)
1.00
C08
C03
C02
C25
C44
C13
C46
C50
C10
Upper
Paleocene
Eocene
Oligocene
Miocene
Pliocene
Pleistocene
Holocene
90
80
70
60
50
40
30
20
10
0 (Ma)

Fig. 4

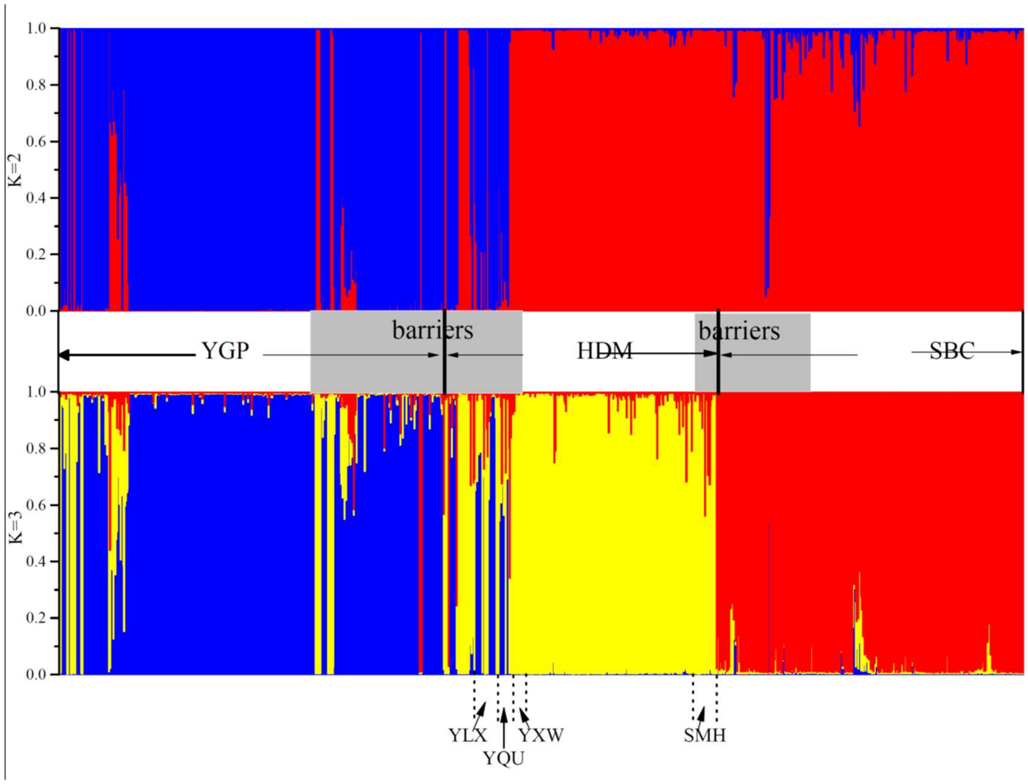
1.0
0.8
0.6
0.4
0.2
0.0
K=2
barriers
YGP
HDM
barriers
SBC
1.0
0.8
0.6
0.4
0.2
0.0
K=3
YLX
YQU
YXW
SMH

Fig. 5

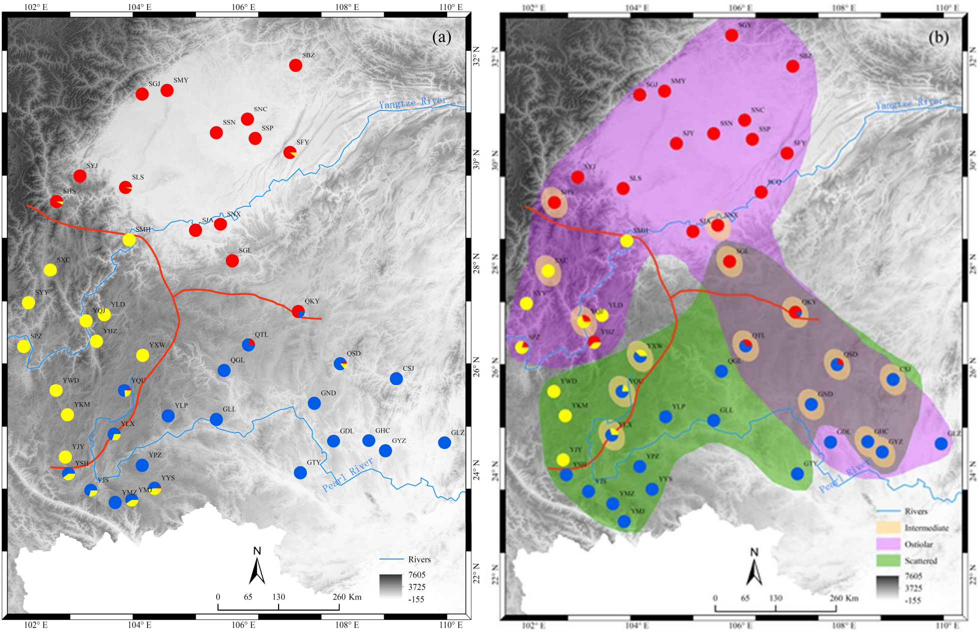
(a)
(b)
102° E
104° E
106° E
108° E
110° E
22° N
24° N
26° N
28° N
30° N
32° N
SGY
SBZ
SGJ
SMY
SNC
SSN
SJY
SSP
SFY
SYJ
SLS
SHS
SCQ
SJA
SNX
SMH
SGL
SXC
SYY
YLD
YQJ
YHZ
SPZ
QKY
QTL
YXW
QSD
QGL
CSJ
YWD
YQU
GND
YKM
YLP
GLL
YLX
GDL
GHC
GYZ
GLZ
YJY
YSH
YPZ
GTY
YJS
YYS
YMZ
YMJ
Yangtze River
Pearl River
N
0
65
130
260 Km
Rivers
Intermediate
Ostiolar
Scattered
7605
3725
-155

Fig. 6

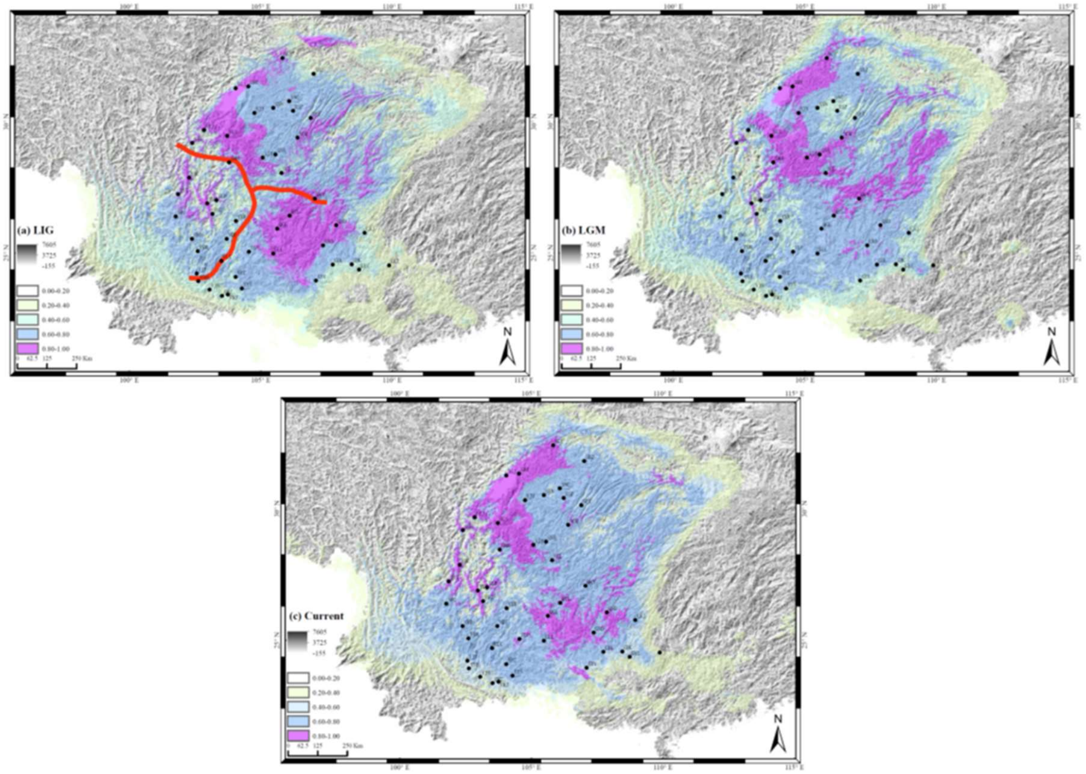
100° E
105° E
110° E
115° E
30° N
25° N
(a) LIG
(b) LGM
(c) Current
7005
3725
-155
0.00-0.20
0.20-0.40
0.40-0.60
0.60-0.80
0.80-1.00
0 62.5 125 250 Km
N

Fig. 7

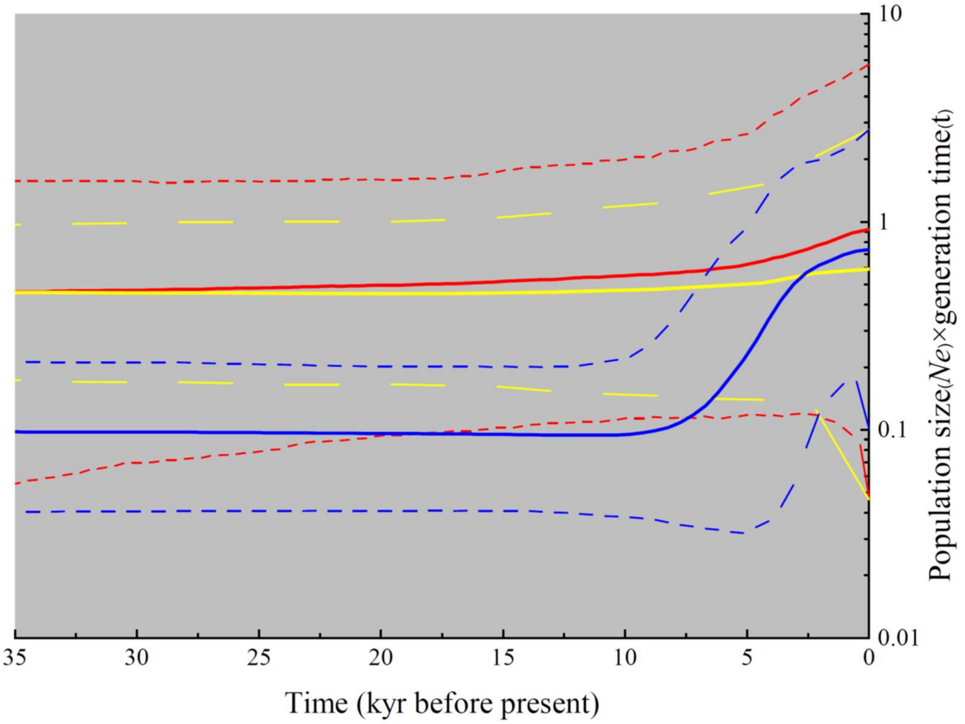
10
1
0.1
0.01
Population size(Ne)×generation time(t)
35
30
25
20
15
10
5
0
Time (kyr before present)

Fig. 8

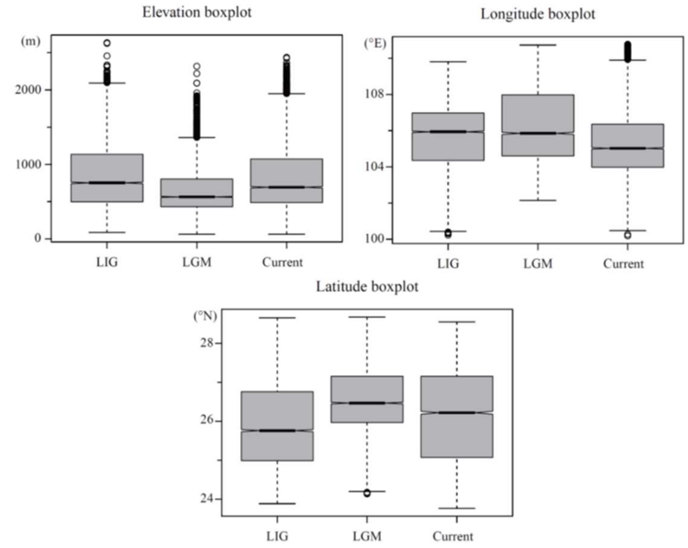
Elevation boxplot

Longitude boxplot

Latitude boxplot